EXPRESSION OF CANDIDATE GENES FOR HORN GROWTH IN EARLY BOVINE DEVELOPMENT

A Thesis

by

SARAH M. VITANZA

Submitted to the Office of Graduate Studies of
Texas A&M University
in partial fulfillment of the requirements for the degree of

MASTER OF SCIENCE

December 2009

Major Subject: Animal Science

EXPRESSION OF CANDIDATE GENES FOR HORN GROWTH IN EARLY BOVINE DEVELOPMENT

A Thesis

by

SARAH M. VITANZA

Submitted to the Office of Graduate Studies of
Texas A&M University
in partial fulfillment of the requirements for the degree of

MASTER OF SCIENCE

Approved by:

Co-Chairs of Committee,	Clare A. Gill
	Penny K. Riggs
Committee Member,	James O. Sanders
Head of Department,	Gary Acuff

December 2009

Major Subject: Animal Science

ABSTRACT

Expression of Candidate Genes for Horn Growth in Early Bovine Development.

(December 2009)

Sarah M. Vitanza, B.S., Texas A&M University

Co-Chairs of Advisory Committee: Dr. Clare A. Gill
Dr. Penny K. Riggs

Bovine horns develop primarily after birth and the presence or absence of horns is due to a single gene. It has been reported that the horn bud appears in the bovine embryo at d 60 of gestation. Our hypothesis is that the gene that determines the presence of horns is expressed in osteoprogenitor cells of the early fetus and will affect the expression of *RUNX2*, *MSX1*, *MSX2*, and/or *TWIST1*.

To test this hypothesis, bovine fetal samples were collected from commercial females at the Caviness Packing Company in Hereford, Texas. Fetuses ranged from d 28 to d 80 of gestation. A survey of the expression of genes from the region on bovine chromosome 1 known to contain the locus that causes horns (*IFNAR1* to *SOD1*), was conducted using qualitative and quantitative RT-PCR, and in situ hybridization. Genes with known roles in osteogenesis and chrondrogenesis (*MSX1*, *TWIST1*, *RUNX2* and *SOX9*) were included as positive controls.

With the exception of *OLIG1*, which was only expressed in the brain, all of the genes investigated were expressed in fetal frontal and parietal bones by qualitative RT-

PCR. The level of expression of *C21orf59*, *C21orf66*, *IL10RB*, and *SFRS15* increased in the frontal bone of horned samples from d 55 to d 70 of gestation.

At d 60 of gestation, a change in the shape of the frontal bone was observed, which has been reported to be the developmental stage when the horn bud appears. At this time point, *MSX1*, *TWIST1*, *RUNX2* and *SOX9* were detected in frontal bone, in cells from the osteoblast lineage, as expected. Furthermore, *C21orf59*, *C21orf62*, *C21or66* and *SFRS15* from the polled interval were localized to developing mesenchyme, osteoblasts and/or osteoclasts of the frontal bone, suggesting that each of these genes has a role in intramembranous bone formation. In addition, gradients of expressed *C21orf66* and *SFRS15* were detected in developing endochondral bone. There was evidence of an antisense transcript of *C21orf66* expressed in the same cell types as the sense transcript. Further characterization of this antisense transcript demonstrated that it covered the entire sense transcript. Based on observed expression in the mesenchyme, rather than just in mature osteoblasts or osteoclasts, *C21orf66* and/or its antisense transcript become the most likely candidates for the polled locus.

DEDICATION

I dedicate this to everyone who has supported me during this process. To Colt, for being by my side through the ups and downs, always encouraging me to do well, listening, and understanding. I couldn't have come this far without you and your encouragement to help me stick to my goals.

ACKNOWLEDGEMENTS

Thanks to my committee chair, Dr. Clare Gill for allowing me to be a student worker and then accepting me as a graduate student. I have learned a lot through her guidance, which has opened doors to new opportunities. I thank Dr. Penny Riggs for serving as a mentor and guiding me through techniques. I would also like to thank Dr. Jim Sanders for his guidance and for serving on my committee.

I would also like to give my great appreciation to Colette Abbey for teaching me lab techniques, and for her guidance and motivation. My time in the lab has been a great joy and has encouraged me to persue an occupation in a professional lab. I would like to acknowledge all my fellow graduate students for helping out and being there when I needed someone.

I would like to give a special thanks to Dr. Brad Lindsey at Ovitra Biotechnology for allowing me to go with him to collect my fetal samples at a commercial packing plant - what an experience. If it was not for him, my project would not be as complete. I would like to thank Dr. Suresh Pillai for allowing the use of the real-time PCR machine, and to Palmy Jesudhasan for his assistance. I am thankful for Dr. Huaijun Zhou and Hsin-I Chiang (Sam) for allowing the use of, and assistance in using, the bioanalyzer and robot. Thanks to Dr. Nancy Ing and Cindy Balog-Alvarez for the use of their histology equipment and their assistance. I would also like to thank Kelli Kochan for her assistance in analysis of real-time data, and a special thanks to Dr. Kathrin Dunlap for

her assistance in histology and overall support. Without the support and kindness of these people, this research would have been very difficult.

To my biggest support, Colt, for your patience and encouragement. Without you I could have not accomplished many of my goals in life. Finally, thanks to my family for their encouragement in my education.

TABLE OF CONTENTS

LIST OF FIGURES

FIGURE Page

LIST OF TABLES

1. INTRODUCTION

Horns cost cattle producers and the meat industry more than an estimated $22 million every year from bruised carcasses and damaged hides. The presence or absence of horns in *Bos taurus* cattle is controlled by an autosomal locus with 2 alleles and the polled phenotype is due to a dominant mutation (Georges et al., 1993). Producers are unable to readily distinguish heterozygous polled animals from homozygous polled animals, thus eradication of horns from a herd can be a time-consuming process. The region known to contain the polled locus is located on bovine chromosome (BTA) 1q12 in the interval from *IFNAR1* to *SOD1* (Figure 1.1; Appendix B), which corresponds to human chromosome (HSA) 21q21-22 and coincides with part of the Down syndrome critical region (Davis et al., 1999).

Horns develop on the frontal bone adjacent to the coronal suture between the frontal and the parietal bone. Recent histological analysis of horn samples from neonatal and 5 to 6 mo old *Bos indicus* influenced cattle provides evidence that horns develop through intramembranous ossification, which is how the flat bones of the skull are formed (Wunderlich, 2008). However, in neonatal samples, none of the genes from the polled critical interval were differentially expressed in skin and horn, suggesting that the polled locus most likely has its primary effect during fetal development (Wunderlich, 2008). The objective of this study is to conduct a survey of gene expression in bovine

---

This thesis follows the style of Journal of Animal Science.

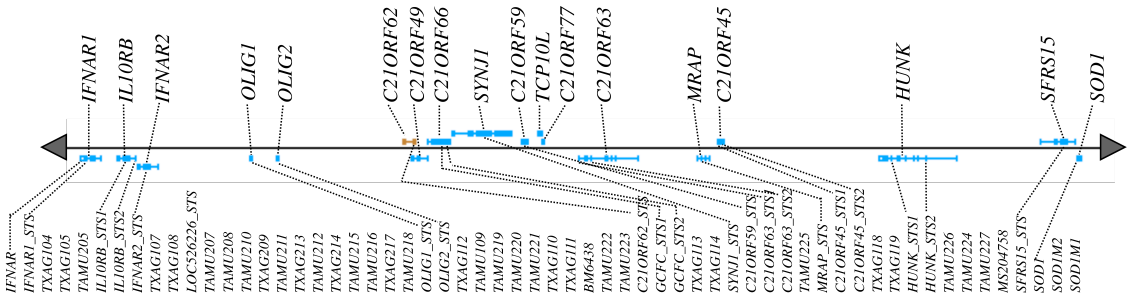

Figure 1.1. Polled interval on bovine chromosome 1. Gene names above the horizontal line are based on human nomenclature. Bovine markers are listed below the line. Region spans from 1,278,530 to 2,920,913 of the Btau4.0 assembly of the bovine genome sequence. Modified from Wunderlich (2008).

fetal samples at various stages of development for genes in the region on BTA1 (*IFNAR1* to *SOD1*) known to contain the locus that causes horns, along with other genes with known roles in the osteogenesis and chrondrogenesis pathways.

2. LITERATURE REVIEW

2.1 Economic Importance

Horns are problematic for cattle producers and the meat industry. More than $22 million is estimated to be lost every year from bruised carcasses and damaged hides due to horns. Bruising was one of the top 10 concerns for beef producers identified in the 2000 National Beef Quality Audit (McKenna et al., 2002). However, in the 2005 National Beef Quality Audit (Smith et al., 2006), the number of horned cattle and carcasses damaged had not changed significantly.

Producers dehorn cattle to alleviate potential damage to other cattle and to prevent harm to caretakers. Dehorning has been one of the main practices used to remove horns but it can cause additional stress to the animal that negatively affects gain (Goonewardene and Hand, 1991), lead to a risk of infection at the wound site, and cause potential injury to caretakers during the dehorning procedure. Producers have moved to using cattle that are polled in order to eliminate the need for dehorning (Goonewardene et al., 1999). Distinguishing homozygous polled from heterozygous polled cattle is difficult for cattle breeders because of the recessive inheritance of the horned allele. Despite efforts to eradicate horns by removal of horned animals, heterozygous polled animals retain the recessive allele and can produce horned offspring. Identification of genetic factors that affect horn growth and development could aid producers to select against horns.

2.2 Horns

The presence or absence of horns in *Bos taurus* cattle is controlled by an autosomal locus with 2 alleles (Georges et al., 1993). The horned phenotype is due to a homozygous recessive gene (pp) (Long and Gregory, 1978) and the polled phenotype is due to a dominant mutation (P).

Additionally, there is a separate gene that causes scurs, which are horn-like growths above the frontal bone in the same location as a horn. The scur phenotype (Sc) appears to be expressed as a sex-influenced trait with incomplete penetrance. Scurs can vary in size from small and scab-like to large and horn-like (Asai et al., 2004). This variation in size makes it difficult for producers and breed associations to correctly classify the polled, scurred and horned phenotypes. Buchanan Smith (1927) proposed that there is a third locus affecting horn growth based on observations in crosses between Aberdeen-Angus bulls and Angoni (a zebu breed) and Mashukulumbwe (Mashona sanga-zebu) cows in Northern Rhodesia (now Zambia), as well as in the Wild White Park cattle that formed the Park Cattle breed. This later became known as the African horn gene (Ha) and is thought to be epistatic to polled in males but not in females and inherited like scurs, in a sex-limited manner (White and Ibsen, 1936). None of these genes have yet been identified.

In 1829, Sandifort reported that the bony core of the horn is a compound structure composed of a frontal outgrowth or pedicle, a superimposed ossification in the cartilaginous matrix, and a frontal sinus that will extend up into the pedicle (cited by Gadow, 1902). In contrast to this, others postulated that the horn is a result of a separate

center of ossification originating in tissues above the periosteum (dermal and subcutaneous connective tissues surrounding bone), which subsequently fuses to the frontal bone and appears as a simple bony growth (Dove, 1935). Based on cases of regrowth following surgical removal of horns, Hoffsis (1995) suggested that the corium, the area of cells located at the junction of the horn and skin, is the primary site of horn growth.

2.3 Cranial Development

Craniofacial morphogenesis is regulated by interactions between the surface and neural ectoderms, endoderm, paraxial mesoderm and cranial neural crest (Francis-West et al., 1998). After migration of neural crest cells has occurred, the mesenchyme of the head develops from the paraxial mesoderm and the cranial neural crest (Noden, 1983). As cranial mesenchymal cells proliferate, causing expansion and increased extracellular space, the neural folds bulge outward to create the head region.

Through a series of experiments, mostly done with a quail-chick chimera culture system, it was determined that the bones of the cranial vault, the overlying periosteum and the intervening sutures are derived from the dermal layer (Noden, 1983). The cranial neural cells migrate to the facial region in response to ecto-mesenchymal interactions (Abzhanov et al., 2007). These cells differentiate into skeletogenic progenitor cells, forming condensations, which then differentiate into osteoblasts. The osteoblasts produce a bone-specific matrix as a scaffold for bone development (de Crombrugghe et al., 2001). In the head, this leads to the development of the cranial bones, which include the frontal bone, parietal bones, temporal bones and occipital bone.

These 4 major bones make up the skullcap and are crucial in normal developing calvaria (skull).

Jiang et al. (2002) utilized a transgenic mouse carrying a permanent neural crest lineage marker and DiI labeling of cranial mesoderm to demonstrate that the murine frontal bone is derived from the cranial neural crest, whereas the parietal bone is derived from mesoderm. Horns develop on the frontal bone adjacent to the coronal suture with the parietal bone, so the finding that these 2 bones are derived from different cell lineages is relevant to the current study.

2.4 Bone Development

Osteogenesis is the formation and development of bone, which occurs by replacing preexisting connective tissue (Kierszenbaum, 2002). There are 2 processes through which bone can develop: 1) intramembranous ossification in which bone is directly made from the mesenchyme, and 2) endochondral ossification, in which there is a cartilage template that is replaced by bone.

Bones of the skull and part of the clavicle are formed by intramembranous ossification, a multi-step process. As the embryonic mesenchyme becomes more vascularized, these cells begin to develop into osteoprogenitor cells, pre-osteoblasts and then mature osteoblasts, which are cuboidal-type cells that produce the osteoid (bone) matrix (Kerr, 1999; Stein et al., 2004). As the matrix becomes mineralized, the osteoblasts become osteocytes linked by canaliculi. Trabeculae are formed from the linked osteocytes, as a radial structure in which hemopoietic tissues allow for blood

supply (Kerr, 1999). As the bone develops it transforms from woven bone to lamellar bone.

Endochondral ossification, a better understood process, gives rise to long bones that become the appendicular skeleton, facial bones, vertebrae, and lateral medial clavicles. Like intramembranous ossification, the initial condensation of mesenchyme and the eventual formation of calcified bone are the same. However, there is an intermediate step in which a cartilaginous template regulates growth and development of the bone (Ornitz and Marie, 2002). Cartilage is needed to lengthen and increase the diameter of rapidly developing bones.

Endochondral ossification occurs within the mesenchyme, as cells begin to proliferate into chondrocytes. Proliferating chondrocytes begin to mature into hypertrophic chondrocytes forming the matrix. As the matrix increases in size, the center becomes calcified. This is the site of bone deposition. The inner perichondral cells develop into osteoblasts and the center becomes a cylindrical collar. As cartilage is removed, blood vessels traffic osteogenic cells to the site to allow for new bone deposits (Kerr, 1999).

It has been described that horns develop via endochondral bone formation through a cartilage matrix; however, little histological data support this hypothesis (Fambach, 1901; Gadow, 1902). After recent histological analysis of neonatal and 5 to 6 month old *Bos indicus* influenced cattle, Wunderlich (2008) proposed that horns develop through intramembranous ossification. Horns develop on the frontal bone adjacent to the coronal suture between the frontal bone and the parietal bone (Wunderlich, 2008).

The roles of these bones and the coronal suture in horn development remain unclear. The sutures between the flat bones of the skull function as the growth centers of the bones. At the edges of these bones are osteogenic fronts that contain highly proliferating cells, which then differentiate (Connerney et al., 2008).

Growth and development of the frontal and parietal bones are regulated by a number of osteogenic genes (Stein et al., 2004). The principal osteogenic marker is runt-related transcription factor 2 (RUNX2, previously known as CBFA1), which is initially observed when pluripotent mesenchymal stem cells are committed to the bone cell lineage prior to formation of the osteoblast (Ducy et al., 1997). Runt-related transcription factor 2 is not only a critical gene for the development of intramembranous bone but also for endochondral bone formation.

The msh homeobox genes 1 and 2 (*MSX1* and *MSX2*) function as transcriptional regulators that control cellular proliferation and differentiation during embryonic development (Hill et al., 1989). Together *MSX1* and *MSX2* have critical roles in craniofacial development and, in particular, in the development of the frontal and parietal bones. Cranial mutations of these genes disrupt the tissue-tissue interactions among the developing bones (Han et al., 2007). Both *MSX1* and *MSX2* are expressed when osteogenic differentiation is visible in the frontal primordium, and *MSX2* is expressed in the parietal primordium.

Twist homolog 1 (TWIST1) is a basic helix-loop-helix transcription factor that organizes the tissue arrangement of cranial mesenchyme (Soo et al., 2002). Twist homolog 1 is strongly expressed in the cranial mesenchyme just beneath the epithelium

(Rice et al., 2000). As the embryo matures, *TWIST1* expression becomes more localized to the calvarial mesenchyme. Osteoblasts grow and differentiate in this area and initiate the development of the frontal and parietal bones. Twist homolog 1 becomes localized to the osteogenic fronts of these bones and affects suture development.

To understand early embryonic development of the bovine horn, it will be necessary to investigate genes that also contribute to the development of the dermal layer, frontal and parietal bones and their sutures. Our hypothesis is that the gene that determines the presence of horns is expressed in osteoprogenitor cells of the early fetus and will affect the expression of *RUNX2*, *MSX1*, *MSX2* and/or *TWIST1*.

3. MATERIALS AND METHODS

3.1 Fetal Collection and Dissection

Bovine fetal samples out of commercial females were collected at the Caviness Packing Company in Hereford, Texas for RNA extraction (n = 20) and histological analysis (n = 8). Fetuses were assigned gestational ages of 28 d to 80 d of gestation based on crown-rump length (Richardson et al., 1991). Those that were d 50 and older were dissected using the ear, eye, and occipital condyle as reference points. An incision was made with a sterile scalpel between the frontal bones from the nasal bones continuing posteriorly to the occipital condyle. A second incision was made from the nasal bones continuing posteriorly just above the eye and ear to meet the first incision at the occipital condyle (Appendix A.1). Using sterile scissors and tweezers, 4 tissues (frontal bone, parietal bone, skin, and brain) were collected for extraction of RNA and directly stored in RNAlater (Invitrogen, Carlsbad, CA) for further processing.

For histology, an incision was made between the frontal and nasal bones splitting the head in half from the occipital condyle to the nose. A second incision was made at the occipital condyle to remove the head. For analysis of the top of the head, an incision was made just above the ears continuing to the front just above the eyes (Appendix A.2). These dissected heads were placed into 4% paraformaldehyde for 12 to 48 hr (approximately 24 hr per 1 cm section).

For the extraction of RNA from fetuses less than d 50 of gestation, an incision was made just behind the occipital condyle cutting through the neck to remove the head.

These heads were dissected prior to RNA extraction into the same 4 tissues as listed above. For histological analysis, whole fetuses were fixed in 4% paraformaldehyde.

To establish the phenotypes of the fetal samples, a set of 44 single nucleotide polymorphisms (SNP) were used in a SNPlex assay (Applied Biosystems) to produce genotypes for the fetuses (n = 20). The genotypes were phased using PHASE v2.1 and the resultant haplotypes were compared to breed-specific haplotypes for 8 *Bos taurus* breeds for these same markers (Clare Gill, pers. comm.).

3.2 Histology

After fixation in 4% paraformaldehyde for 12 to 48 h, samples were rinsed in 50% ethanol and then in 70% ethanol for 8 to 24 h each, with final storage in 70% ethanol until further processing. Samples were embedded in paraffin and sections were cut to a thickness of 7 μm for histology and *in situ* hybridization. Embedding and hematoxylin and eosin staining were performed by the Texas A&M Department of Veterinary Integrative Biosciences Histology Laboratory.

3.3 RNA Extraction

RNA was extracted in Trizol reagent (Invitrogen, Carlsbad, CA) with the addition of 1-Bromo-3-chloro-propane (BCP) (Sigma, St. Louis, MO). Approximately 50 to 100 mg of tissue was cut into small pieces using sterile scissors and quickly transferred into a pre-chilled mortar containing liquid nitrogen, ground into a fine powder with a pre-chilled pestle, then transferred to a 15 ml conical tube containing 2.2 ml of Trizol. The tissue was homogenized 6 to 8 times with an 18 gauge needle and a sterile syringe, transferred to two 1.5 ml microcentrifuge tubes, and centrifuged at

14,000xg for 5 min at 4°C to remove cell debris. The homogenate was incubated at room temperature for 5 min to promote dissociation of nucleoprotein complexes. The supernatant was transferred to a new 1.5 ml tube containing 200 µl BCP, shaken vigorously for 15 s, incubated at room temperature for 3 min and centrifuged at 12,000xg for 10 min at 4°C. The upper aqueous phase containing RNA was transferred to a new 1.5 ml tube containing 200 µl BCP and 400 µl Trizol, shaken vigorously for 15 s, incubated at room temperature for 3 min and centrifuged at 12,000xg for 10 min at 4°C. The upper aqueous phase was again transferred to a new 1.5 ml tube containing 200 µl BCP, shaken for 15 s, and centrifuged at 12,000xg for 10 min at 4°C. The aqueous layer was then transferred to a new 1.5 ml tube and 1 volume of isopropanol was added to precipitate the RNA. Samples were washed in 70% ethanol, then resuspended in nuclease free water.

The RNeasy Mini Kit (Qiagen, Valencia, CA) was used to complete purification of total RNA according to the manufacturer's instructions. Samples were treated with 27 Kunitz units of DNase 1 on the RNeasy column. After washing the column with 350 µl of RW1 Buffer and 500 µl RPE Buffer, 50 µl of RNase-free water was added directly to the spin column, and centrifuged at 8,000xg for 1 min to elute the RNA. This was repeated using the eluate to increase RNA concentration. RNA samples were stored at -80°C.

Total RNA was quantified on a Nanodrop ND-1000 spectrophotometer (Nanodrop Technologies, Wilmington, DE). RNA quality for qualitative reverse transcriptase polymerase chain reaction (RT-PCR) was assessed by capillary

electrophoresis on an RNA 6000 NanoChip with a 2100 Bioanalyzer (Agilent Technologies, Palo Alto, California). Based on Nanodrop concentrations, a nanochip was used to assess RNA with concentrations of greater than 100ng/µl, and a picochip was used for those with concentrations less than 100ng/µl. Samples with an RNA Integrity Number (RIN) less than 5.0 were excluded.

3.4 Primer Design

Primers for qualitative RT-PCR (Table 3.1) were from Wunderlich (2008). In addition, for quantitative RT-PCR, most of the primers were from Wunderlich (2008). In those cases where primer design was required, sequence data available from NCBI (http://www.ncbi.nlm.nih.gov) and UCSC Genome Bioinformatics (http://genome.ucsc.edu) were used. Primers were designed using Primer3Plus software (http://www.bioinformatics.nl/cgi-bin/primer3plus/primer3plus.cgi). Criteria were an optimal melting temperature of 58°C and maximum of 63°C; self-complementarity of 8 bases; 3' end self-complementarity of 6 bases; product length of 50 to 120 base pairs (Table 3.2). Primers were aligned against the bovine (Btau 4.0) or human genome sequences using the BLAST algorithm to ensure orthologous genes were being investigated. Primer pairs were also checked using the In silico PCR tool at UCSC to verify that they were expected to produce a unique amplicon based on the Btau 4.0 assembly of the bovine genome sequence.

3.5 Polymerase Chain Reaction

Polymerase Chain Reaction (PCR) was used to optimize primers and to determine qualitative analysis of gene expression. Various annealing temperatures

Table 3.1. Gene-specific primers used for qualitative RT-PCR[1]

Primer	Forward	Reverse	gDNA (bp)[2]	cDNA (bp)[3]	T_A (°C)[4]
C21orf45	CGGATTGTTGTGAAGGATGT	ACAGCGTAGCAAGATGCAGT	323	323	57
C21orf59	CCATCATTAGCAGCGAGGAG	GGCAAACTTCATCTGGGTCT	425	187	58
C21orf62	AACAGAGTTTGCTCATCCAC	GGCACAGCTACGATATTAGTAA	263	263	55
C21orf63.1	TGACCATCAGTTGCTAATC	GCTGACAATGACTCCATCTT	1825	115	55
GAPD_quant	TTCAACGGCACAGTCAAGG	ACATACTCAGCACCAGCATCAC	237	119	60
HUNK	TTGATGGAACATGCCAGAAC	TCTGAATCTGCGTGATGAGC	373	373	57
IFNAR1	GTGGTCATTTATGTTGTGAGC	GAAGTGGAAAGGAGTAGATTCC	1357	131	55
IFNAR2	CTGTCAGTCTGGGTGTTTGC	CGTTAGTCCATGCTTGGTGT	177	177	55
MRAP	CATCTGGAGGCAACCCAG	CTCCCATCGAGAGGTTCTGT	234	234	58
OLIG1	GGCGCAAGATCAACAGC	CCAGCAGCAGGATGTAGTTG	174	174	60
SYNJ1	AGTTGCAATACGAATGCTGT	TGCTGTCTGATAAGCTCTTTC	470	234	64
SOX9[5]	TGCTCAAGGGCTACGACTG	CGAGATGTGCGTCTGTTCC	788	358	64

[1] Wunderlich (2008)
[2] gDNA = Expected size in genomic DNA
[3] cDNA = Expected size in complementary DNA
[4] Annealing temperature
[5] Not in the polled interval but involved in chondrogenesis and osteogenesis

Table 3.2. Gene specific PCR primers for real-time RT-PCR

Role	Primer	Forward	Reverse	Size (bp)
Polled Interval	C21orf45[1]	GAGCTGGGTGGCGAGTCA	TGTTCCTCATTCACAGAAACATTACA	80
	C21orf59[1]	GGCGCAGCGCATCTG	TCATCAGTCAGTCCTTGCATATTAGG	83
	C21orf62[1]	TGGGCACAGCTTCTTTCTGA	CCTCTGAGCTCTGGTGAAGCA	69
	C21orf66[1]	CATGCCAAACGTCGGATTG	CAAGGTGATCTGCCATCTTACCA	68
	IL10RB[1]	CACCTTCTGTCCTGTGGATGAC	AACGCACATGTAAAGAATTAGCAAGT	57
	SFRS15[1]	CACCTCCACCTCCAGTTAAAGTTT	TGGGCAACTGCGGTACAGT	72
	SYNJ1[1]	GAATGCTGTTCCACACCACAA	TTTCGTTCTTTGACTTGGGATTG	54
Osteogenesis/ Chondrogenesis	BMP4	AACACCGTGAGGAGCTTCCA	TGCTGAGGTTAAAGAGGAAACGA	94
	BMP7.2	AGCTGAGTTCCGCATTTACA	AGCTGAGTTCCGCATTTACA	87
	COL18A1[1]	GATCCATGGGCACTTCTTCAG	TCCACCAGCATCTGGTACGT	61
	CYR61	TTACAGTTGGGCTGGAAACT	GCTCTGAAGGGGATCTGC	98
	FGFR2_exon6	CTTTTCCACGTGTTTGATCC	TGGAGTTTGTCTGCAAAGTG	68
	FGFR2_exon7	CACGTATATTCCCCAGCATC	CACGTATATTCCCCAGCATC	70
	FGFR2_exon8	TTCTTGGTCGTGTTCCTCAT	CATAGGGGTGTTCTTCATCG	72
	FIGF	CGCCATCCATTCTCAATTAT	AGGACAGAGCTTCTTGGAA	82
	FOXL2[1]	CTCACGCTGTCCGGCATCT	CGTAGAACGGGAACTTGGCTATAAT	52
	GREM1	TGACCCTCTTCTTCTTGGTG	TTTCAGTCCTGCTCCTTTTG	100
	MSX2	CTGGTCAAACCCTTCGAGAC	GAGTATCTGCCCGGTTCC	64
	PRKAC[1]	GGACCTGAAGCCAGAGAACCT	TTCACACGCTTGGCGAAC	80
	PTHLH[1]	AACATCGCTGGAGCTCAACTC	CCTGCAATACGTCTTCTGAAGGT	70
	RUNX1[1]	GGGAGCTGCTTGCTGAAGAT	ACAACAAGCCGATTGAGTTAGGA	82

Table 3.2 continued.

Role	Primer	Forward	Reverse	Size (bp)
Osteogenesis/ Chondrogenesis	RUNX2[1]	CCAACCCACGAATGCACTATC	AGGGACATGCCTGAGGTGACT	66
	SOX9[1]	AATCTCCTGGACCCCTTCATG	GGCGGACAGGCCCTTCT	57
	STAT1[1]	GCCTCTATCCTGTGGTACAACATG	ACAAGGTGGGTTCAGGAAGAAG	68
	TINP1	ACATGAGCCTTCTTGAAACG	TGGCTTTACTCGAAAACCAC	75
	TWIST1[1]	AGCAGAACCCAAATTCAAAGAAAC	TGCCCGTCTGGGAATCAC	92
	TWIST2[1]	CGACGAGATGGACAATAAGATGAC	CACACGGAGAAGGCGTAGCT	75
	18S[1]	AGAAACGGCTACCACATCCA	CACCAGACTTGCCCTCCA	169
	YWHAZ[1]	GCATCCCACAGACTATTT	GCAAAGACAATGACAGACCA	120

[1]Wunderlich, 2008

(50 to 64°C) and magnesium concentrations (1.5 mM to 3.5 mM) were tested to optimize primers until a single amplicon was obtained by PCR (40 ng genomic DNA template, 0.2 μM forward and reverse primer, 0.12 mM dNTPs, 1U Taq polymerase, 1X Buffer (50 mM KCl, 10 mM Tris-HCl, pH 9.0, 0.1% Triton X-100)). Thermal cycling was performed on a MJ PTC-200 (MJ Research, Waltham, MA) thermal cycler (95°C for 5 min; 35 cycles at 95°C for 30 sec, and annealing temperatures ranging from 50-64°C for 30 sec, 72°C for 30 sec; 72°C for 7 min). Amplicons were separated by size on an agarose gel (2% or 3% agarose, 1X TAE, 0.2 μg/ml ethidium bromide) and visualized under ultraviolet light (302 nm). Gels were photographed with a Kodak DC290 digital camera and the 1D image analysis software (Eastman Kodak Co., Rochester, NY). After primers were optimized, they were used to survey gene expression qualitatively with cDNA as the template.

3.6 Reverse Transcriptase Polymerase Chain Reaction

For qualitative assessment of mRNA, reverse transcription (RT) was performed using the SuperScript™ II Reverse Trancriptase Kit with Oligo(dT) primers (Invitrogen, Carlsbad, CA) according to the manufacturer's instructions. DNase treated RNA samples (500 ng) were used as the template for the reaction. Following transcription, 2 μl of the synthesized cDNA was used as template for PCR. Genomic DNA, an RT negative, and a template negative control were also included for each PCR reaction. Amplification of *GAPDH* was used as a positive control. Amplicons were separated by agarose gel (2% or 3% agarose, 1X TAE, 0.2 μg/mL ethidium bromide) electrophoresis, visualized under ultraviolet light (302 nm), and photographed using a Kodak DC290

digital camera with the 1D image analysis software (Eastman Kodak Co., Rochester, NY). Gene expression was qualitatively determined by the presence or absence of amplicons on these agarose gels.

For quantitative assessment of mRNA, reverse transcription was performed using the SuperScript^{TM} VILO cDNA Synthesis Kit with random hexamers (Invitrogen, Carlsbad, CA) according to the manufacturer's instructions. DNase treated RNA samples (60 ng) were used as the template for the reaction. Following transcription, the newly synthesized cDNA was diluted 1 to 20 in 25ng/µl of tRNA (Invitrogen, Carlsbad, CA). A 2 µl aliquot of diluted cDNA was used as template for quantitative RT-PCR (qRT-PCR) utilizing SYBR GreenER qPCR SuperMix (Invitrogen, Carlsbad, CA). Samples were loaded into a 384-well optical PCR plate (catalog # MPS-3898, Phenix, Hayward, CA) using an Eppendorf epMotion 5070 robot (Eppendorf, Westbury, NY). Plates were then sealed with optical PCR sealing tape (catalog # LMT-OPCT, Phenix, Hayward, CA) and loaded onto an ABI 7900HT real-time PCR machine (Applied Biosystems, Foster City, CA) for thermal cycling (60°C for 2 min, 95°C for 10 min, 40 cycles at 95°C for 15 sec and 60°C for 1 min) utilizing SDS 2.3 software (Applied Biosystems, Foster City, CA), although analysis was done using SDS 2.2 software. Due to the limited amount of RNA available from the fetal samples, only one biological and one technical replicate was used on each plate, and 18S rRNA and *YWHAZ* were used for normalization.

For primers not previously optimized, RNA was serially diluted in 10-fold increments from 0.6 µg/µl to 0.00006 µg/µl, followed by reverse transcription. Realtime

qRT-PCR assays were used for further analysis if assay efficiency was within the range of 90% to 100% efficient. Dissociation curve analysis was used to verify presence of a single PCR product.

To assess the existence of sense and antisense transcripts, reverse transcription was performed with the SuperScript^{TM} III First-Strand Synthesis System for RT-PCR Kit (Invitrogen, Carlsbad, CA) with gene-specific primers (GSP; Table 3.3) according to the manufacturer's instructions. DNase treated RNA samples (500 ng) from horn buds (n = 5) or skin (n = 5) of neonates or 5 mo old calves were used as templates along with 2 µM GSP for each reaction. Forward and reverse GSP were used separately in the reverse transcription reaction with the same samples as template to produce sense and antisense transcripts. Complementary DNA was diluted 1 to 10 in DEPC-treated water. A 3 µl aliquot of the diluted cDNA was used as a template for PCR, along with genomic DNA, an RT negative, and a template negative control. Pairs of GSP were used to amplify the cDNA. The presence or absence of a band was visualized under ultraviolet light (302 nm) after electrophoresis on agarose gel (3% agarose, 1X TAE, 0.2 µg/ml ethidium bromide). Amplicons from cDNA reverse-transcribed from the forward primer correspond to an antisense transcript and amplicons derived from reverse-transcription with the reverse primer correspond to a sense transcript.

Table 3.3. Primers for each exon of *C21orf66*[1]

Primer	Forward	Reverse	Size (bp)	T_A (°C)[2]
C21orf66_EXON1_3	GGTAGCTGGGAAAGGGAAAC	TCCTCCTCCGAGTCATTCC	199	63
C21orf66_EXON2	TGAAGAAATCAAGTTACAGCAA	GTCGGCAGATGAGTTGAGTT	190	58
C21orf66_EXON3	CAAAGCAGGTCATGTTAAGGA	CCTTTGGCTTTTCTTCTTCC	110	58
C21orf66_EXON4	GGGAATTGGGAGATTTCACT	GGCGTTTCTCATCATCATCT	108	50
C21orf66_EXON5	TGATGATGACGCTCTGGTAA	TATCTGCTCCTGTTCCCATC	67	58
C21orf66_EXON6	CAATGCCTTATGGTTCATCC	GGGAGTTTTGAAAGGGACTG	107	58
C21orf66_EXON7	CAGGGCCATTGAGAGATTAG	ACATACCCTCGCATTTCTTG	81	58
C21orf66_EXON7alt	GCAAGTGTCCTGACAGCATA	ACATACCCTCGCATTTCTTG	226	58
C21orf66_EXON8	AGCTGTACAAACAGCGAGCT	AGCTGTACAAACAGCGAGCT	87	58
C21orf66_EXON8alt	AGCTGTACAAACAGCGAGCT	GGACTGACTTGAATGGCTTG	95	58
C21orf66_EXON9	CTCTGATGGCACCAAATCTT	ACGTTTGGCATGTTCTTGAT	68	58
C21orf66_EXON10	TCGTAGACAAGCCAGAGAGC	CTTCAAGGTGATCTGCCATC	50	58
C21orf66_EXON11	GCCTGGCGTTCAAAATACTA	TTATGAGGGGGTTGAGCAG	82	58
C21orf66_EXON12	GCTGTGGTTTGAATCTTTGC	CATCGACATCGTCCTTTTCT	68	58
C21orf66_EXON13	ATGTGGGACCCCTTTTCTAC	TTTTCTGCATTCACCACTGA	95	58
C21orf66_EXON15	AAAAATTCTGGGCCTTACTTG	AACTGAAGACCAAAACTGTCG	51	58
C21orf66_EXON16	GGTATGGCATTTTCTCAAACA	TTTTGATGCTGTCATCTCCA	116	58
C21orf66_EXON17	AGCAGTGGTTCGTGAATCTT	CATCAGAGCACCCAATACTG	117	58
C21orf66_EXON18	GTGTTCGAGCTCTGGATCAT	TTCACATTGTGGTCACTTGC	52	58

[1] Exon 14 was too small to design effective primers, thus this exon was amplified using exon 13 forward and exon 15 reverse
[2] Annealing temperature

3.7 Analysis of Real-Time Reverse Transcriptase Polymerase Chain Reaction

Realtime data were analyzed by relative quantification (Livak and Schmittgen, 2001). The geometric means of the C_t values for *18S* and *YWHAZ* were used as the reference genes for normalization, and the mean of frontal and parietal bone samples from polled fetuses was used as the calibrator.

3.8 Periodic Acid-Schiff Reaction

Slides were prepared for staining by melting wax at 55°C for 10 to 15 min. Sections were dewaxed using Citrisolv (Fisher, Atlanta, GA) for 5 min 3 times each and then hydrated in 100% and 95% ethanol twice for 1 min and then in 70% ethanol for 3 min. Slides were rinsed twice in double distilled water for 1 min. Slides were then placed in 0.5% periodic acid (Sigma, St. Louis, MO) for 5 min then rinsed in double distilled water twice. Slides were stained in Schiff's reagent for 15 min at room temperature, and then washed in running tap water for 10 min to develop color. Slides were then stained in Mayer's Hematoxylin for 2 min and washed in running tap water for 2 min to develop color. Slides were then dehydrated in 70% ethanol for 3 min and 95% and 100% for 1 min 2 times each. Slides were in placed in Citrisolv (Fisher, Atlanta, GA) for 5 min 3 times. Slides were mounted in Permount (Fisher, Fair Lawn, NJ), coverslipped and allowed to dry overnight.

3.9 Probe Design

Primers were designed to produce amplicons 300 to 500 bp in length, which were then optimized using cDNA from tissues known to express the genes of interest (Table 3.4). Amplicons were cloned into the PCRII vector using the PCRII dual promoter TA

cloning kit (Invitrogen, Carlsbad, CA). Amplicons were ligated in a 1:1 molar ratio with the PCR2 vector at 14°C overnight, transformed into TOP10F' competent cells by heat shock, and plated on LB-agar plates containing 100 µg/ml Ampicillin, 0.05 mg/ml IPTG, and 0.04 mg/ml X-gal and grown at 37°C overnight. White colonies were selected from the agar plates and used to inoculate 5 ml LB containing 100 µg/ml Ampicillin. Cultures were grown at 37°C overnight with shaking at 250 rpm on a ThermoForma model 420 orbital shaker (Thermo Electron Corporation, Marietta, OH). After a 16 to 20 hr incubation, 500 µl of culture was mixed with 500 µl 2X freezing solution (72 mM K_2HPO_4, 26 mM KH_2PO_4, 3.4 mM sodium citrate, 0.8 mM $MgSO_4$, 13.6 mM $(NH_4)_2SO_4$, 8.8% glycerol) to produce a glycerol stock which was stored at -80°C. A dilution of the glycerol stock was used directly in PCR as described above with universal PUC forward (GTTTTCCCAGTCACGAC) and reverse (CAGGAAACAGCTATGACC) primers to determine orientation of the insert and to ensure amplicon identity.

The PCR product was purified using Princeton Separations (Adelphia, New Jersey) PSIclone HTS 96-well PCR clean-up plate kit as per the manufacturer's instructions. Sequencing reactions were performed using 60 ng of this purified PCR product, 0.5 µM PUC forward or reverse primer and 2 µl of Big Dye v1.1 Terminator mix (PE Corp. Applied Biosystems, Foster City, California). The template, primer and water were mixed and denatured at 98°C for 2 min, followed by snap cooling on ice for 2 min. The Big Dye was then added and the reaction was cycled 25 times at 96°C for 10 seconds, 50°C for 5 seconds, and 60°C for 4 min.

Table 3.4. Gene specific primers used to develop probes for *in situ* hybridization

Primer	Forward	Reverse	Size (bp)
C21orf59[1]	GGCTCAACGTCATCAAAGAA	GGCAAACTTCATCTGGGTCT	343
C21orf62[1]	AACAGAGTTTGCTCATCCAC	GGCACAGCTACGATATTAGTAA	263
C21orf66[1]	GATGTCGATGTCGCACTGTT	CTGCATTCACCACTGAAGGA	166
MSX1	GAGTTCTCCAGTTCGCTCAG	TGTCAGGTGGTACATGCTGT	300
RUNX2[1]	CGAAATGCCTCTGCTGTTAT	TACTGAGAGTGGAAGGCCAG	322
SFRS15[1]	AGTTCGTGTATTGAACCTTTG	GGTACAGTTGGTACAGAGTTTG	201
SOX9[1]	TGCTCAAGGGCTACGACTG	CGAGATGTGCGTCTGTTCC	358
TWIST1[1]	TCCAGAGAAGGAGAAAATGG	GTCCATAATGATGCCTTTCC	360

[1] Wunderlich (2008)

Dye terminator and salts were removed from the sequencing reactions using Qiagen's DyeEx kit as per the manufacturer's instructions. Cleaned sequences were dried down, resuspended in 10 µl di-formamide and loaded onto an ABI 3130xl (Applied Biosystems, Foster City, California) using 50 cm capillaries and POP7 polymer with an injection rate of 1.6kV for 15 s, and electrophoresed at 8.5kV.

Plasmid DNA was isolated using the Plasmid Maxi-kit (Qiagen, Valencia, CA) according to the manufacturer's instructions. Plasmid DNA (~20 µg) was digested with 50 U *BamHI* (Promega, Madison, WI) or *EcoRV* (Promega, Madison, WI) at 37°C overnight. After digestion, an equal volume of phenol:chloroform:isoamyl alcohol (25:24:1) was added to the digest, vortexed, and centrifuged at 8000xg for 5 min. The upper aqueous phase was removed to a clean tube and an equal volume of chloroform was added, vortexed, and centrifuged at 8000xg. The upper aqueous phase was transferred to a clean tube and DNA was precipitated with 1/10 volume 2M NaCl and 2.5 volumes of absolute ethanol at -80°C for 1 hr. Samples were centrifuged at 13000xg for 10 min, rinsed with 70% ethanol, air dried and then re-suspended in 50 µl sterile water. DNA was quantified on a Nanodrop ND-1000 spectrophotometer (Nanodrop Technologies, Wilmington, DE) and run on an agarose gel (1% agarose , 1X TAE, 0.2 µg/ml ethidium bromide) to ensure complete digestion.

3.10 Labeling with Digoxigenin

Probes for *in situ* hybridization were labeled with digoxigenin-UTP by in vitro transcription using the DIG RNA Labeling (SP6/T7) kit (Roche, Indianapolis, IN) according to the manufacturer's instructions. The T7 promoter was used for *BamHI*

digests and SP6 promoter for *EcoRV* digests to obtain antisense and sense probes dependent on the orientation of the insert. Probes were purified using Centri-Sep columns (Princeton Separations, Inc., Adephia, NJ). Dot blots were used to the determine labeling efficiency of the probes (Roche, Indianapolis, IN) by immunological detection using the Roche DIG Nucleic Acid Detection kit (Roche, Indianapolis, IN) in accordance with the product manual, except volumes were reduced to 10 to 20 ml dependent on the size of the blot. Based on these results, probes were diluted to a working concentration of 10 ng/µl.

3.11 In situ Hybridization with Poly d(T)

The mRNA integrity of the sections was verified by the use of a Poly d(T) Probe and Novocastra™ Detection Kit (Leica Microsystems, United Kingdom). Slides were prepared for hybridization by melting wax at 55°C for 10 to 15 min. Sections were then dewaxed using Citrisolv (Fisher, Atlanta, GA) 2 times for 3 min each and then hydrated in 100% ethanol twice for 3 min and in 95% ethanol once for 3 min. Slides were then rinsed in DEPC-treated water for 3 min, covered with 100 µl of 5 µg/ml of Proteinase K (0.05 M Tris-HCL pH7.6) and incubated for 30 min at 37°C. Slides were then rinsed twice in DEPC-treated water for 3 min and then dehydrated in 95% and 100% ethanol for 3 min each. Slides were allowed to air dry before adding 20 µl of the probe hybridization solution from the kit. Sections were then coverslipped, placed in a humid chamber at 65°C for 15 min, and allowed to incubate at 37°C for 2 hr. Sections were then washed in TBS (50 mM Tris-HCl pH 7.6, 150 mM NaCl) containing 0.1% Triton 3 times for 3 min each. Slides were placed on an incubation tray and covered with 100 µl

of blocking solution (normal rabbit serum diluted 1:5 in TBS, 3% w/v BSA, 0.1% v/v Triton) for 10 min. Blocking solution was tipped off and sections were covered with 100 µl of 1:200 antibody solution (Rabbit F(ab') anti-FITC in TBS, 3% w/v BSA, 0.1% v/v Triton) for 30 min. Slides were washed twice in TBS for 3 min and in alkaline phosphatase substrate buffer (0.1 M Tris-HCl, pH 9.5, 0.1 M NaCl, 50 mM $MgCl_2$) for 5 min. Sections were covered in 100 µl of color solution from the kit, coverslipped, sealed with rubber cement, and placed in a humid chamber protected from light overnight. Coverslips were removed and slides were washed in running tap water for 5 min and mounted with Clear Mount (Electron Mircoscopy Sciences, Hatfield, PA). The integrity of mRNA was determined by viewing sections with and without probe under bright field on a Nikon Eclipse E1000 microscope to evaluate the intensity of purple staining due to hybridization of the poly d(T) probe to polyA mRNA.

3.12 In situ Hybridization Using Digoxigenin-Labeled Probes

Slides were prepared for hybridization by melting wax at 55°C for 10 to 15 min. Sections were then dewaxed in 3 changes of Citrisolv (Fisher, Atlanta, GA) for 5 min each with agitation every 2 to 3 min. Rehydration was done through a series of 100%, 95%, and 70%, ethanol washes; each wash was for 2.5 min and repeated twice. Sections were then rinsed in DEPC-treated water for 2 min each, then twice in DEPC-1X PBS for 5 min and treated in DEPC-1X PBS with 0.3% Triton X-100 (Fisher, Atlanta, GA) for 15 min. Sections were then rinsed twice in DEPC-1X PBS for 5 min and permeabilized in 5 µg/ml proteinase K in TE for 10 min. Sections were post fixed in DECP-1X PBS with 4% paraformaldehyde at 4°C for 5 min, and then rinsed twice in DEPC-1X PBS for

5 min. Sections were then treated twice in DEPC-1X PBS with 100 mM glycine for 3 min and then rinsed twice in DEPC-1X PBS for 5 min. Sections were acetylate treated in 0.1 M TEA plus 0.25% v/v acetic anhydride twice for 5 min and rinsed twice in DEPC-1X PBS for 5 min. Slides were incubated at 37°C for 1 hr in pre-hybridization solution (50% formamide, 4X SSC). Sections were covered with 60 µl of hybridization buffer (40% deionized formamide, 10% dextran sulfate, 1X Denhardt's solution, 4X SSC, 10 mM DTT, 1 mg/ml yeast t-RNA, 1 mg/ml denatured and sheared salmon sperm) containing 10 ng DIG-labeled RNA probe. These sections were then coverslipped, sealed with rubber cement, and placed into a humid chamber at 50°C or 55°C overnight, depending on the probe. Coverslips were removed by immersing slides into 2X SSC for 5 min at room temperature, and then washed twice in 2X SSC for 15 min with shaking at 37°C. Single-stranded RNA was then digested in NTE buffer (500 mM NaCl, 10 mM Tirs pH 8.0, 1 mM EDTA) containing 20 µg/ml RNase A for 30 min at 37°C, followed by 2 washes in 1X SSC for 15 min with shaking at 37°C. Sections were washed in buffer 1 (100 mM Tris-HCl pH 7.5, 150 mM NaCl) at room temperature for 5 min, followed by adding 100 µl of blocking solution (buffer 1 containing 0.1% Triton, 2% normal sheep serum) directly to each section for 15 to 30 min. Blocking solution was decanted and sections were covered with 75 µl of 1:500 antibody solution (buffer 1 containing 0.1% Triton, 1% normal sheep serum, 0.15 U anti-DIG alkaline phosphatase per section), coverslipped and placed in a humid chamber for 2 hr at room temperature. Coverslips were then removed and sections were washed twice in buffer 1 for 10 min, and then twice in detection buffer (0.1 M Tris-HCL pH 9.5, 0.1 M NaCl, 50

mM $MgCl_2$) for 10 min. Sections were then covered with 75 to 100 µl color solution (1 ml detection buffer, 20 µl Roche NBT/BCIP solution, 1 mM levamisole), coverslipped, sealed with rubber cement, and placed in a humid chamber overnight protected from light. Slides were washed and coverslips removed in buffer 3 (10 mM Tris-HCl pH 8.1, 1 mM EDTA) for 5 min, and then rinsed in water for 2 min. Sections were then mounted with Clear Mount (Electron Mircoscopy Sciences, Hatfield, PA) and allowed to dry.

4. RESULTS AND DISCUSSION

4.1 Qualitative Analysis of Gene Expression

The horn bud in cattle appears at d 60 of gestation (Evans and Sack, 1973). In order to refine the list of candidate genes for horn bud formation, the presence or absence of expression of genes from the polled interval (*IFNAR* to *SOD1*) was characterized in bovine fetal frontal bone, parietal bone, skin, and brain samples ranging from d 35 to 75 of gestation (Tables 4.1 - 4.4). Initially, we intended to survey all 19 of the genes from the polled interval in this way (based on Table 4.1 in Wunderlich, 2008), but limited amounts of RNA from the fetal samples led us to change strategy and switch to characterization of expression of a subset of genes by quantitative RT-PCR (Section 4.2, below).

As expected, all tissues expressed *GAPDH*, which was used as a positive control, and *SOX9*, which is involved in chondrogenesis and osteogenesis. Also as expected, *OLIG1* was only expressed in the brain (Table 4.1). However, expression of *OLIG1* was not observed in brain samples from d 50 and d 55 of gestation. *C21orf63*, which is an uncharacterized protein coding gene, exhibited the same expression profile as *OLIG1* in the brain (as well as being expressed in the other tissues). Oligodendrocyte transcription factors 1 and 2 are known to promote oligodendrocyte formation in the central nervous system and Cheng et al. (2007) recently showed that bone morphogenetic proteins (BMP) 2 and 4 repress *OLIG1* and *OLIG2*, which inhibits oligodendrocyte differentiation. Therefore, it is possible that between d 50 and 55 of gestation, BMP signaling is enhanced, thus inhibiting *OLIG1* expression but future studies would be

necessary to verify this hypothesis. Because *OLIG1* expression was limited to the brain, it was not pursued further in the current study.

All of the other tested genes from the polled interval were expressed in each of the tissues at most of the fetal developmental time points sampled. This is in contrast to the results of Wunderlich (2008), which showed by qualitative RT-PCR that expression of *IFNAR1*, *IFNAR2*, *C21orf62*, *C21orf63*, *MRAP*, *C21orf45*, and *HUNK* was not detectable in skin and bone samples from neonates. In neonates, *SYNJ1* was only detected in horned samples.

4.2 Real-Time Reverse Transcriptase PCR

Wunderlich (2008) concluded that *IL10RB*, *SFRS15*, *C21orf66*, *OLIG1*, *OLIG2*, and *HUNK* were candidates for the polled locus based on their expression patterns in neonates and 5 to 6 mo old calves. In the current study, relative levels of expression of 3 of these genes (*IL10RB*, *SFRS15*, and *C21orf66*), plus 4 genes (*C21orf45*, *C21orf59*, *C21orf62*, and *SYNJ1*) from the qualitative study described in Section 4.1 were characterized by real-time quantitative RT-PCR in bovine fetal frontal and parietal bones. RNA extractions from the majority of the skin samples and some brain samples had RIN < 5.0 and were not of sufficient quality to use for quantitative RT-PCR.

To compare relative levels of expression between samples representing the horned and polled phenotypes, we attempted to classify the fetuses based on breed-specific SNP haplotypes. Unfortunately, because most of the cows were probably crossbreds, phenotypes could only be definitively established in a few cases.

Table 4.1. Qualitative assessment of gene expression in bovine fetal brain

	Days of Gestation[1]								
Gene[2]	35	40	45	50	55	60	65	70	75
C21orf45	+	+	+	+	+	+	+	+	+
C21orf59	+	+	+	+	+	+	+	+	+
C21orf62	+	+	+	+	+	+	+	+	+
C21orf63	+	+	+	-	-	+	+	+	+
HUNK	+	+	+	+	+	+	+	+	+
IFNAR1	+	+	+	+	+	+	+	+	+
IFNAR2	+	+	+	+	+	+	+	+	+
MRAP	+	+	+	+	+	+	+	+	+
OLIG1	+	+	+	-	-	+	+	+	+
SYNJ1	NA	+	-	NA	NA	+	+	NA	NA
SOX9	NA	+	+	NA	NA	+	+	+	+

[1] NA = No data available because of limited RNA for samples from these time points
[2] All genes except *SOX9* are from the polled interval. *SOX9* is involved in chondrogenesis and osteogenesis.

Table 4.2. Qualitative assessment of gene expression in bovine fetal frontal bone

	Days of Gestation[1]								
Gene[2]	35	40	45	50	55	60	65	70	75
C21orf45	+	NA	+	NA	NA	+	+	+	NA
C21orf59	+	NA	+	NA	NA	+	+	+	NA
C21orf62	+	NA	+	+	NA	+	+	+	NA
C21orf63	+	+	+	+	-	+	+	+	-
HUNK	+	-	+	NA	NA	+	+	+	NA
IFNAR1	+	NA	+	+	+	+	+	+	+
IFNAR2	+	NA	+	+	+	+	+	+	+
MRAP	+	NA	+	NA	NA	+	+	+	+
OLIG1	-	-	-	-	-	-	-	-	-
SYNJ1	+	NA	+	NA	NA	NA	NA	NA	NA
SOX9	+	NA	+	NA	NA	-	+	NA	NA

[1] NA = No data available because of limited RNA for samples from these time points
[2] All genes except *SOX9* are from the polled interval. *SOX9* is involved in chondrogenesis and osteogenesis.

Table 4.3. Qualitative assessment of gene expression in bovine fetal parietal bone

	Days of Gestation[1]								
Gene[2]	35	40	45	50	55	60	65	70	75
C21orf45	+	NA	+	NA	NA	+	+	+	NA
C21orf59	+	NA	+	NA	NA	+	+	+	NA
C21orf62	+	NA	+	+	+	+	+	+	+
C21orf63	+	+	+	+	-	+	+	-	-
HUNK	+	-	+	NA	NA	+	+	+	NA
IFNAR1	+	NA	+	+	+	+	+	+	+
IFNAR2	+	NA	+	+	+	+	+	+	+
MRAP	+	NA	+	NA	NA	+	+	+	+
OLIG1	-	-	-	-	-	-	-	-	-
SYNJ1	+	NA	+	NA	NA	+	+	NA	NA
SOX9	+	NA	+	NA	NA	+	+	NA	NA

[1] NA = No data available because of limited RNA for samples from these time points
[2] All genes except *SOX9* are from the polled interval. *SOX9* is involved in chondrogenesis and osteogenesis.

Table 4.4. Qualitative assessment of gene expression in bovine fetal skin

	Days of Gestation[1]								
Gene[2]	35	40	45	50	55	60	65	70	75
C21orf45	+	NA	+	NA	NA	+	+	+	+
C21orf59	+	NA	+	NA	NA	+	+	+	+
C21orf62	+	NA	+	+	-	+	+	+	+
C21orf63	+	+	+	-	+	+	-	-	+
HUNK	+	-	+	NA	NA	+	+	-	+
IFNAR1	+	NA	+	+	+	+	+	+	+
IFNAR2	+	NA	+	+	+	+	+	+	+
MRAP	+	NA	+	NA	NA	+	+	+	+
OLIG1	-	-	-	-	-	-	-	-	-
SYNJ1	+	NA	+	NA	NA	+	+	NA	NA
SOX9	+	NA	+	NA	NA	+	+	+	+

[1] NA = No data available because of limited RNA for samples from these time points
[2] All genes except *SOX9* are from the polled interval. *SOX9* is involved in chondrogenesis and osteogenesis.

Among the fetuses collected, 2 were classified as polled (2.55 and 5.70) and 2 horned (5.55 and 1.70), while phenotypic classification of the remaining samples based on their genotypes was inconclusive. Therefore, the real-time RT-PCR results presented in Figures 4.1 to 4.3 must be treated as descriptive only because they are based on a single biological sample for each phenotype from each time point (d 55 and 70 of gestation).

Expression of *SYNJ1* was not detected in the samples evaluated. Given that expression of *SYNJ1* was observed in the qualitative study (Section 4.1), it may be necessary to redesign the primers used for real-time analysis to confirm this negative result. Similarly, *C21orf45* and *C21orf62* were not evaluated because amplification was inconsistent and these primers would need to be redesigned to characterize expression of these genes.

C21orf59, *C21orf66*, *IL10RB*, and *SFRS15* (Figure 4.1) from the polled interval and *BMP4*, *TWIST1*, *RUNX1*, and *RUNX2* (Figure 4.2), which have known roles in osteogenesis, showed a general trend that as age increased from d 55 to 70 of gestation, the levels of expression increased in the frontal and parietal bones of fetuses genotyped as horned. In the horned samples, expression of genes from the polled interval tended to be higher in the frontal bone than in the parietal bone, whereas the converse was observed for *TWIST1*, *RUNX1* and *RUNX2* and there was no difference in the level of expression of *BMP4*. Expression of *MSX2* and SOX9 in the parietal bone also increased from d 55 to d 70 (Figure 4.3). There was little variation in the levels of *TWIST2*, except in the frontal bone at d 70 where there was 5.2 fold higher expression in the horned

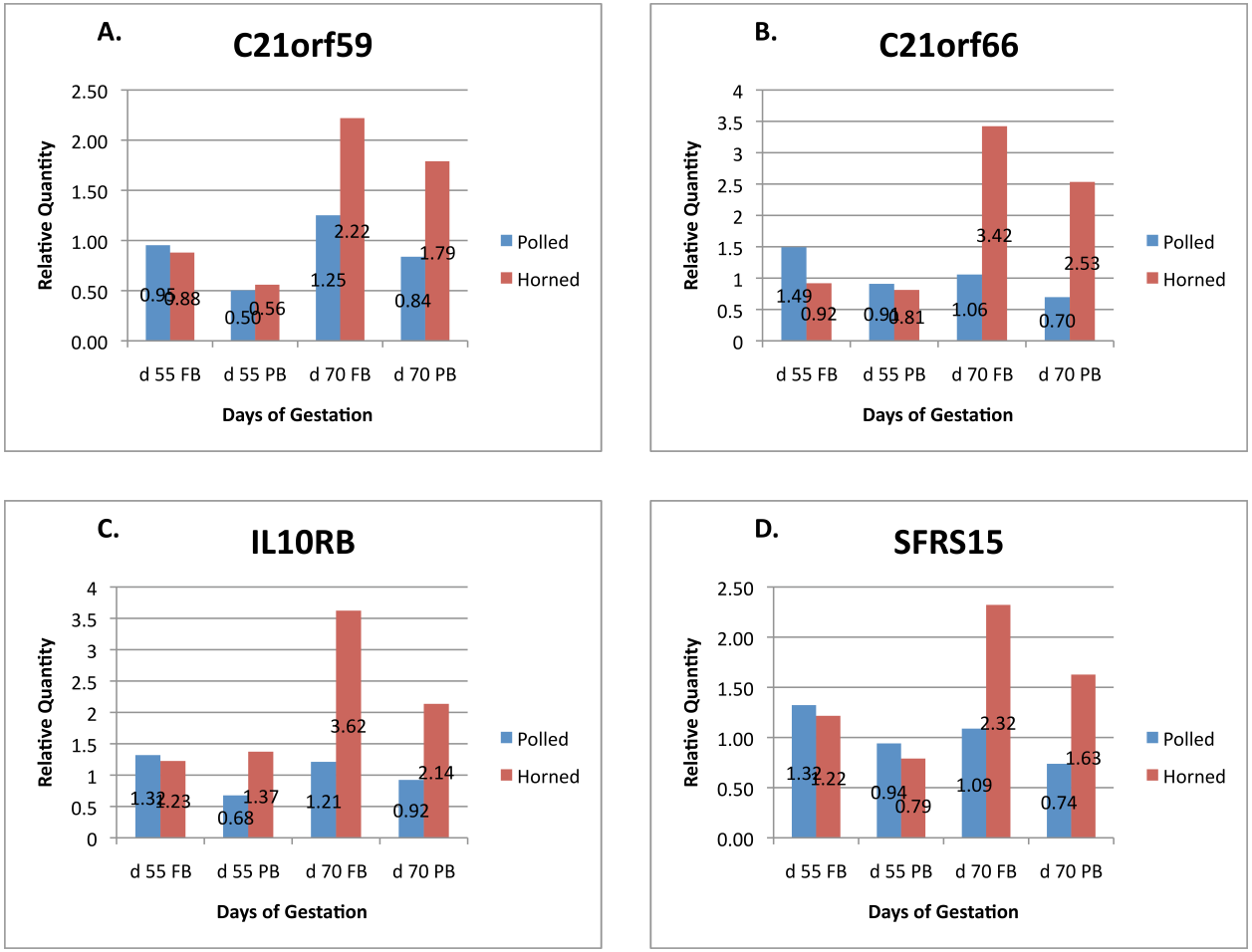

Figure 4.1. Relative levels of expression of genes from the polled interval. Expression was measured in samples from the frontal (FB) and parietal bones (PB) of horned and polled fetuses at d 55 and 70 of gestation.

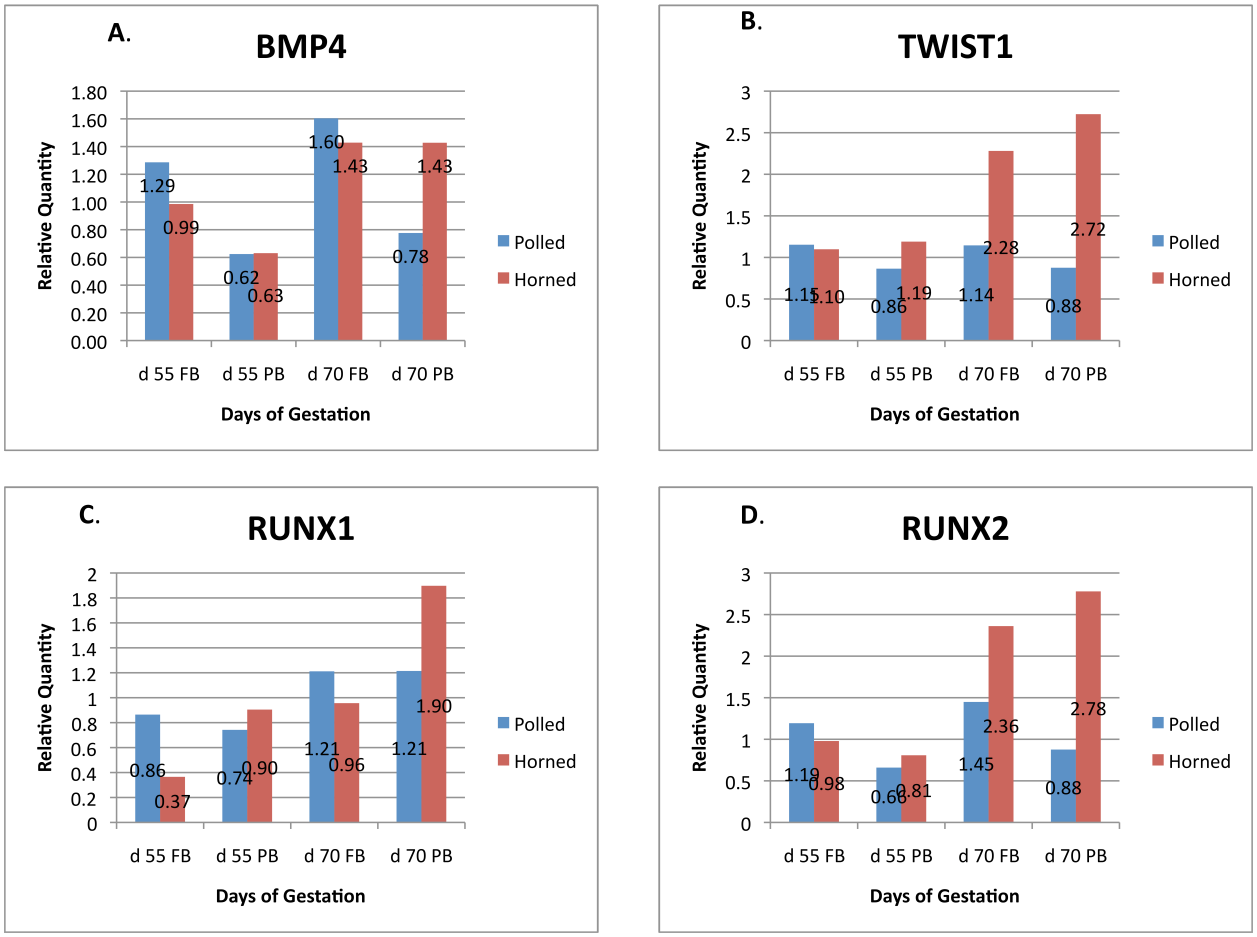

Figure 4.2. Relative levels of expression of genes with known roles in osteogenesis. Expression was measured in samples from the frontal (FB) and parietal bones (PB) of horned and polled fetuses at d 55 and 70 of gestation.

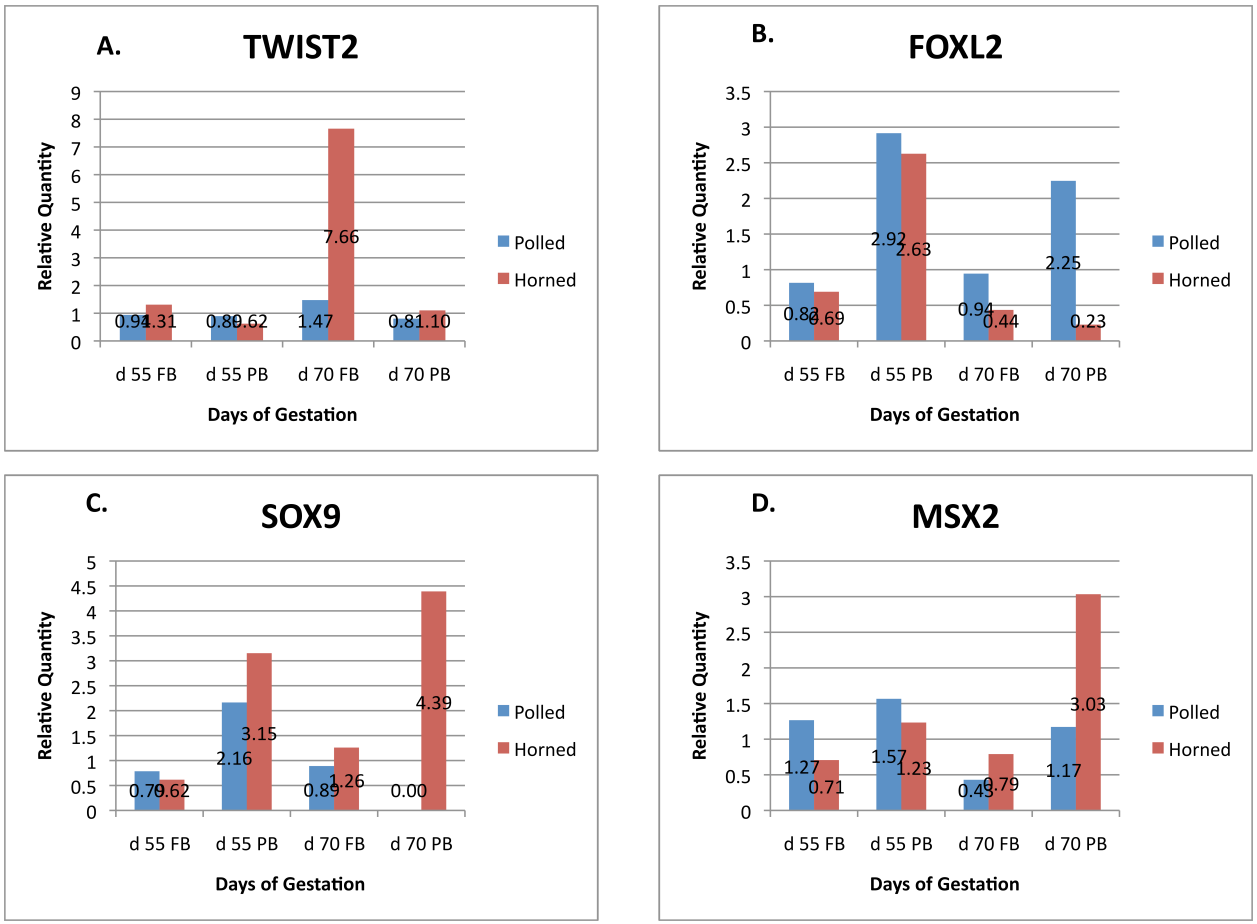

Figure 4.3. Relative levels of expression of genes with known roles in osteogenesis and chondrogenesis. Expression was measured in samples from the frontal (FB) and parietal bones (PB) of horned and polled fetuses at d 55 and 70 of gestation.

sample than the polled sample. Forkhead box L2 was more strongly expressed in the parietal bone than frontal bone and polled samples had higher levels of expression of *FOXL2* than horned samples. However, in the horned samples, expression was 11.4 fold higher in the parietal bone at d 55 than at d 70 (Figure 4.3).

Because of the limited number of samples for which the horned or polled phenotypes could be assigned, and since the frontal and parietal bones consist of a variety of cell types at the developmental time-points sampled, conclusions are difficult to draw based solely on these real-time RT-PCR data. It may be necessary to use laser capture microdissection in future studies to characterize the levels of expression of genes in specific cell types. In this study, *in situ* hybridization (section 4.4) was used as a more specific measure of when, and in which populations of cells, the genes were expressed.

4.3 Microscopic Observation of Periodic Acid-Schiff Reaction

As intramembranous ossification occurs, embryonic mesenchyme becomes the vascularized connective tissue of the periosteum or the pericranium, which covers the outer surface of the skull bones (Figure 4.4). The pericranium is made up of 2 layers; the fibrous layer and the osteogenic layer. The osteogenic layer contains progenitor cells that develop into osteoblasts, which give rise to bone matrix leading to the subsequent development of trabecular bone.

At d 55 and 60 of gestation, the Periodic Acid-Schiff reaction outlined the frontal and parietal bones, evidenced by the dark pink staining in the pericranium of both bones (Figure 4.4). The clear outline of the 2 bones allowed visualization of the coronal

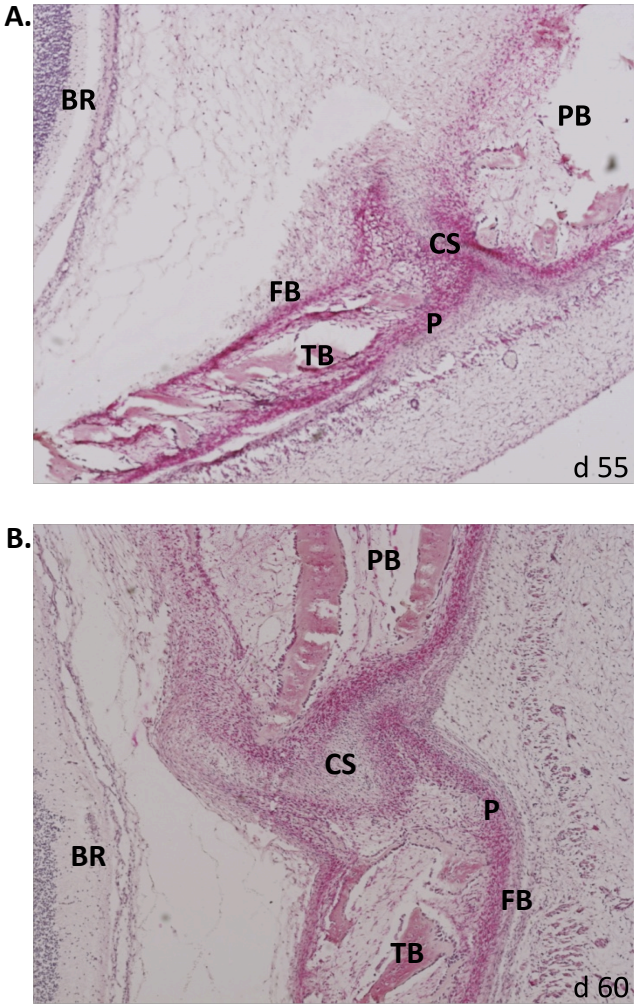

Figure 4.4. Periodic Acid-Schiff reaction in the frontal and parietal bones at the coronal suture at d 55 and 60. Cytoplasm, pericranium, trabecular bone, and osteoblasts are stained pink and the nuclei are stained blue. **A.** Fetus (2.55) genotyped as homozygous polled at d 55. The frontal bone is smooth and flat at the coronal suture as shown by the pericranium in dark pink. **B.** Heterozygous fetus (7.60) at d 60. The frontal bone is curved like a crescent at the coronal suture also shown by the pericranium in dark pink. FB = frontal bone, PB = parietal bone, CS = coronal suture, P = pericranium, TB = trabecular bone, BR = brain. (4X)

suture. Horns grow on the frontal bone adjacent to the coronal suture that is between the frontal and parietal bones, suggesting the suture may have a role in horn development.

Trabecular bone can also be seen within the pericranium. Osteoblasts lining the outside of the trabecular bone, as well as osteocytes within, can be observed. The Periodic Acid-Schiff reaction allowed identification of specific cell types within regions of interest. This provided an anatomical guide for evaluation of the localization of gene expression by *in situ* hybridization.

4.4 *In situ Hybridization*

In situ hybridization was conducted on fetal sections that ranged from d 40 to 80 of gestation in 5 day increments. Probes were for *C21orf59*, *C21orf62*, *C21orf66*, and *SFRS15* from the polled interval, as well as *MSX1*, *RUNX2*, *SOX9* and *TWIST1* that have known roles in osteogenesis, chondrogenesis and suture development. Whereas overall temporal and spatial expression patterns differed for each gene, an unexpected result was that all 4 of the genes from the polled interval were detected in active osteoblasts surrounding newly formed bone, suggesting that each of the genes has a role in intramembranous bone formation.

Examination of whole mounts revealed expression of *RUNX2* and an antisense transcript of *C21orf66* in the developing frontal bone at d 40 and 45, respectively (Figure 4.5). Expression of *C21orf59*, *C21orf62*, *MSX1* and *TWIST1,* in patterns similar to *RUNX2*, was also detected at d 45 (data not shown). Expression of *RUNX2* was limited to osteoprogenitors and osteoblasts, whereas *Anti-C21orf66* was also detected in mesenchymal cells. However, it was difficult to maintain the integrity of the dermal

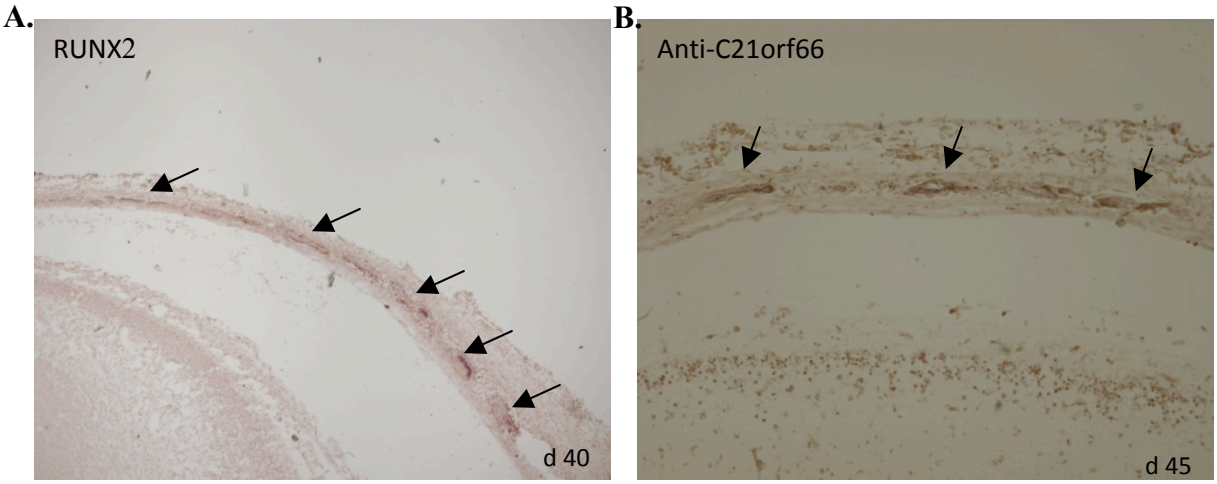

Figure 4.5. *In situ* hybridization of developing mesenchyme at d 40 and 45. **A.** *RUNX2*; (40X) **B**. *Anti-C21orf66;* (100X). Localization of signal to mesenchymal, osteoprogenitor and osteoblast cells is indicated by arrows.

layer in these experiments, and pairs of antisense and sense slides were not obtained. To improve integrity of the sections at these early stages, thicker sections may be needed. Nevertheless, based on this observed expression in the mesenchyme (rather than osteoblasts), *C21orf66* and/or its antisense transcript become the most likely candidate for the polled locus.

As previously shown in Figure 4.4, the frontal bone, near the coronal suture, is curved like a crescent at d 60, which coincides with when the horn bud appears. This region was evaluated for each of the genes (Figure 4.6 - 4.12).

Runt-related transcription factor 2 was abundantly expressed at d 60, whereas *SOX9* was barely detectable (Figure 4.6). Expression of *RUNX2* and *SOX9* was localized to the osteoblasts lining the trabecular bone within the frontal bone and *RUNX2* was also expressed in the developing mesenchyme and along the osteogenic layer of the pericranium.

Runt-related transcription factor 2 determines the osteoblastic lineage of mesenchymal cells (Otto et al., 1997) and regulates osteoblastic proliferation (Lana-Elola et al., 2007), whereas *SOX9* has a well-characterized role in chondrogenesis (Bi et al., 1999) and has also been shown to have a role in early osteogenesis (Yamashiro et al., 2004). The coordinate expression of these genes is crucial for the development of the cranium. Abundant expression of *RUNX2* is not unexpected due to its role in controlling osteoblast maturation and is consistent with the results of Holleville et al. (2007) in E12 chick embryos.

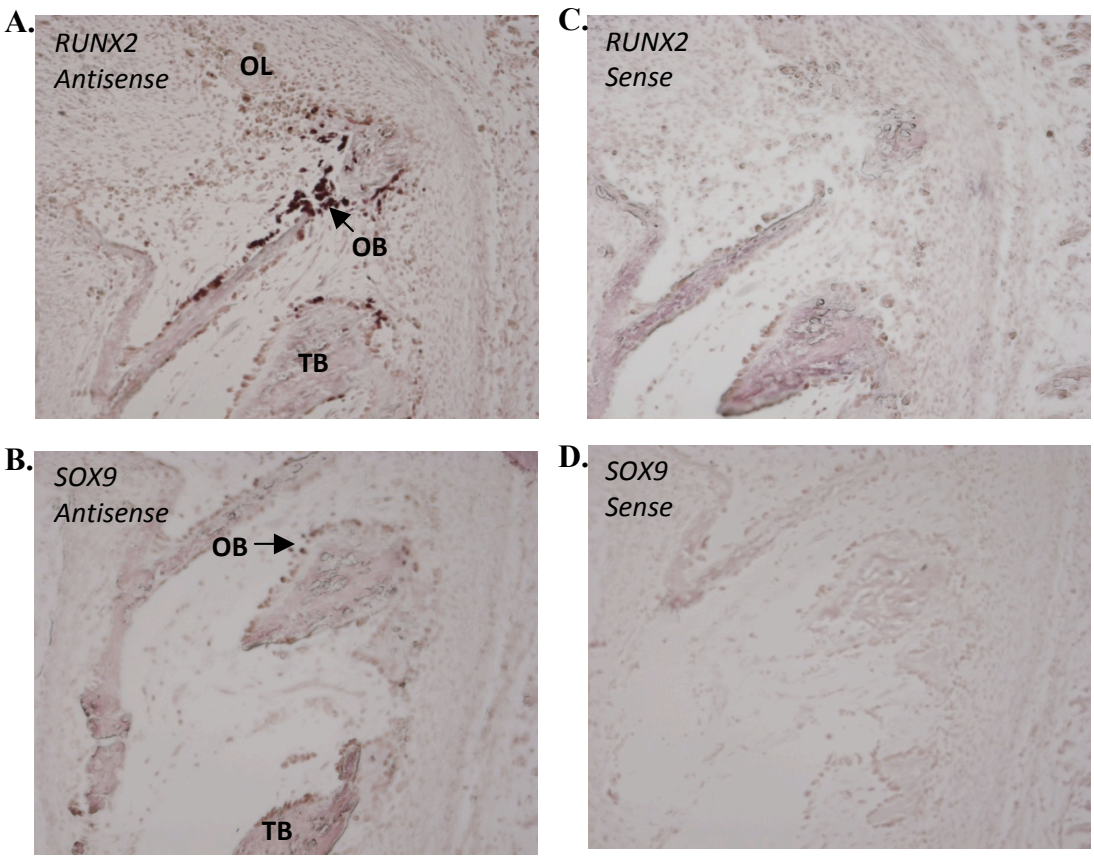

Figure 4.6. Brightfield micrographs of the localization of *RUNX2* and *SOX9* in frontal bone at d 60 of gestation. **A-B.** Hybridization of digoxygenin-labeled antisense probes to sense transcripts. **C-D.** Sense controls. **A, C.** *RUNX2*. Expression was detected in osteoblasts and mesenchyme along the osteogenic layer of the pericranium. **B, D.** *SOX9.* Expression was observed in the osteoblasts lining the trabecular bone. OB = osteoblasts, TB = trabecular bone, OL = osteogenic layer. (40X)

In addition to their roles in craniofacial bone formation, *RUNX2* and *SOX9* are critical for the development of endochondral bones (Stein et al., 2004). For example, expression of *SOX9* was detected in cartilage of the developing knee, foot, spinal column, and rib cage at d 40 and 45 of gestation but there was no evidence of expression in cartilage from the head (data not shown).

At d 55, 60, 75 and 80 of gestation, the transcription factors *MSX1* and *TWIST1* were abundantly expressed in developing mesenchyme, osteoblasts, and osteocytes of the frontal and parietal bones (Figure 4.7), which is consistent with results of Yoshida et al. (2005), Han et al. (2007), and Connerney et al. (2008). These genes were evaluated because they are known to have roles in the development of the osteogenic fronts associated with the coronal suture between the frontal and parietal bones (Ishii et al., 2003; Antonopoulou et al., 2004). Expression of both genes was also detected in the orbital bone (Figure 4.8).

Expression that was restricted to the developing mesenchyme, osteoblasts, and osteocytes was also detected using the *MSX1* sense control probe. This result can be explained because *MSX1* is known to have an antisense transcript that is thought to be involved in autoregulation of the sense transcript (Petit et al., 2009). It is also important to note that while the general levels of expression were similar based on the intensity of hybridization signal, there was a difference in distribution of expression with *MSX1* appearing to be more highly expressed in the mesenchyme toward the suture than *TWIST1*.

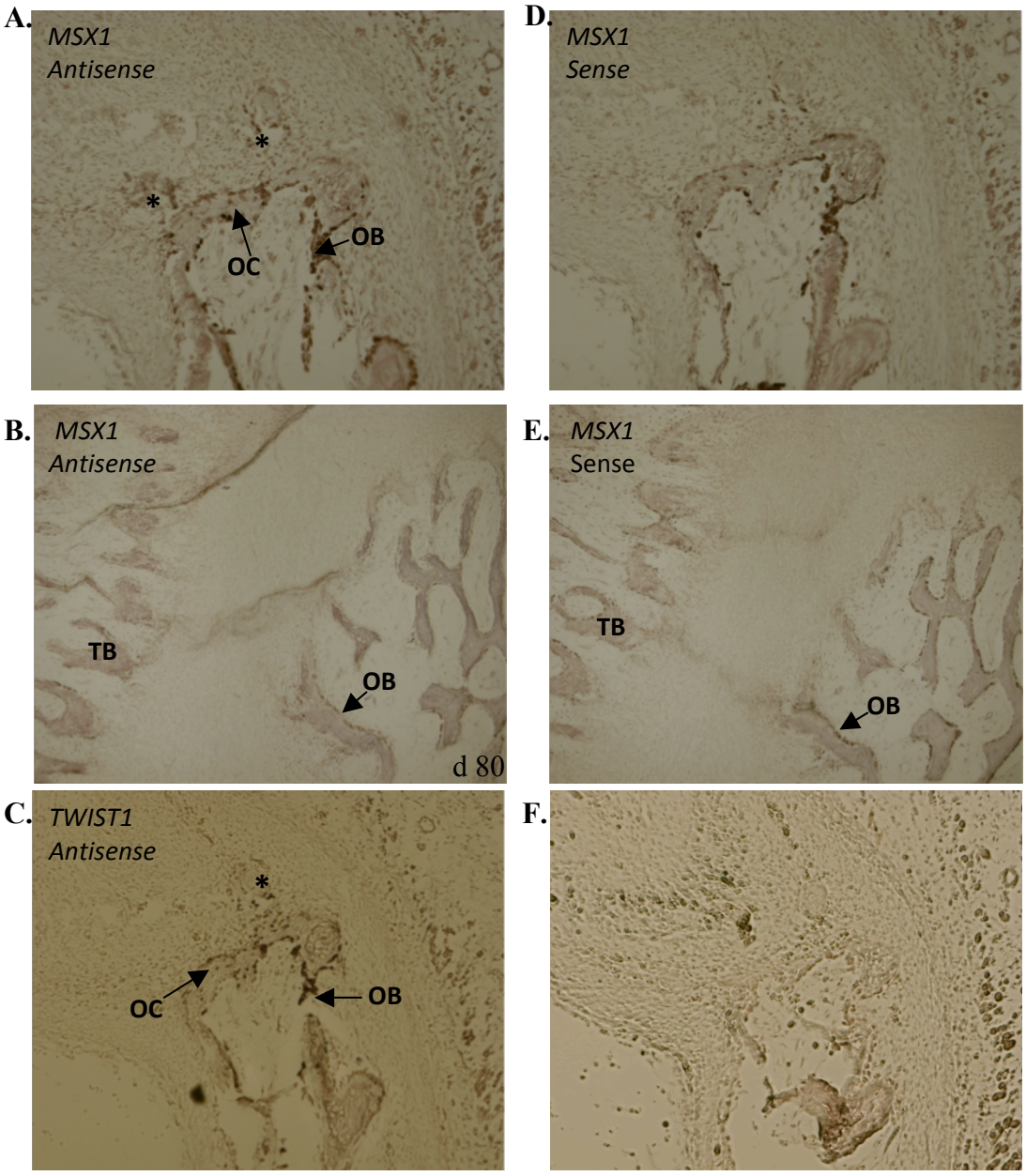

Figure 4.7. Brightfield micrographs of the localization of bidirectional transcripts of *MSX1* and *TWIST1* in frontal bone at d 60 of gestation. **A-C.** Hybridization of digoxygenin-labeled antisense probes to sense transcripts. **D-F.** Sense controls. **A, B.** *MSX1*. Expression was detected in developing mesenchyme (asterisk), osteoblasts and osteocytes. **D, E.** *Anti-MSX1*. The antisense transcript co-localized with the sense transcript. **C, F.** *TWIST1*. Expression was observed in developing mesenchyme, osteoblasts and osteocytes. OB = osteoblasts, OC = osteocytes, TB = trabecular bone. (40X)

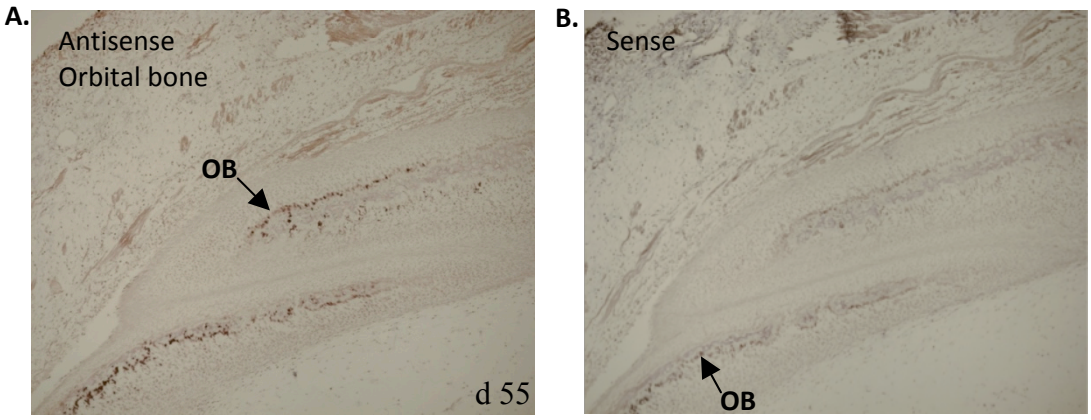

Figure 4.8. Brightfield micrographs of the localization of bidirectional transcripts of *MSX1* in orbital bone at d 55 of gestation. **A.** Hybridization of digoxygenin-labeled antisense *MSX1* probe to sense transcripts. **B.** *Anti-MSX1*. Expression was detected in the osteoblasts. (40X)

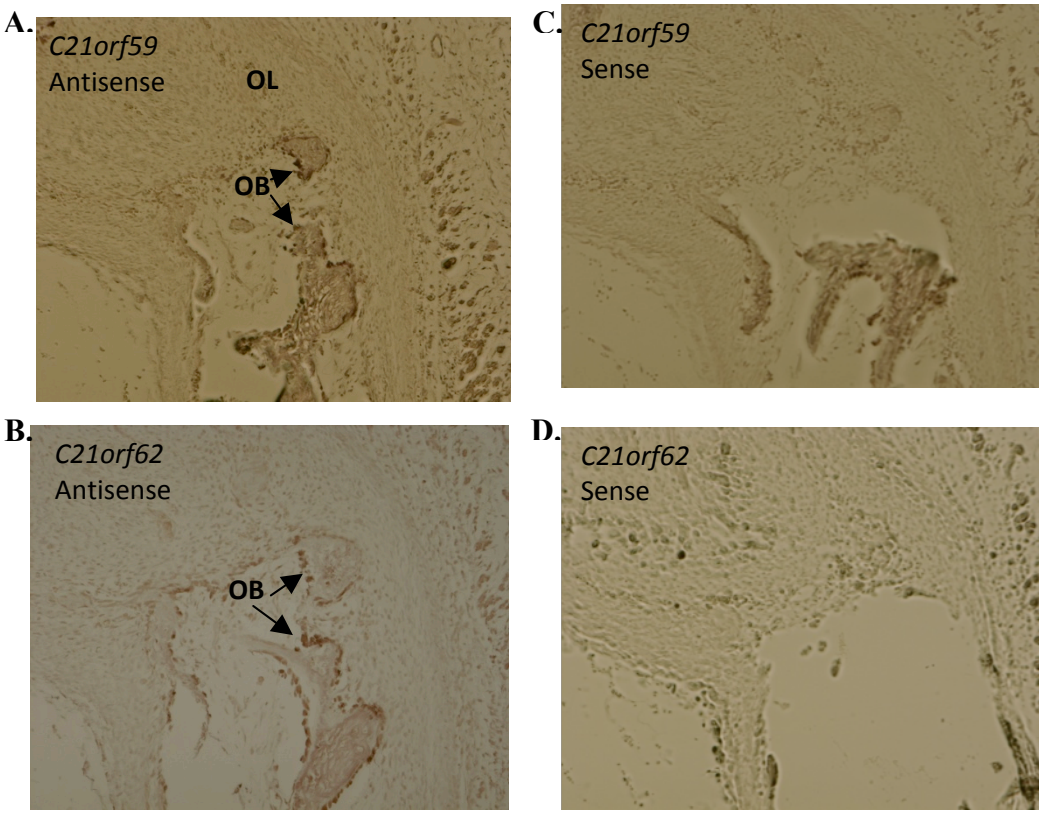

Figure 4.9. Brightfield micrographs of the localization of *C21orf59* and *C21orf62* in frontal bone at d 60 of gestation. **A-B.** Hybridization of digoxygenin-labeled antisense probes to sense transcripts. **C-D.** Sense controls. **A, C.** *C21orf59*. Expression was detected in the osteoblasts lining the trabecular bone and extending into the mesenchyme along the osteogenic layer. **B, D.** *C21orf62.* Expression was observed in osteoblasts lining the trabecular bone. OL = osteogenic layer, OB = osteoblasts. (40X)

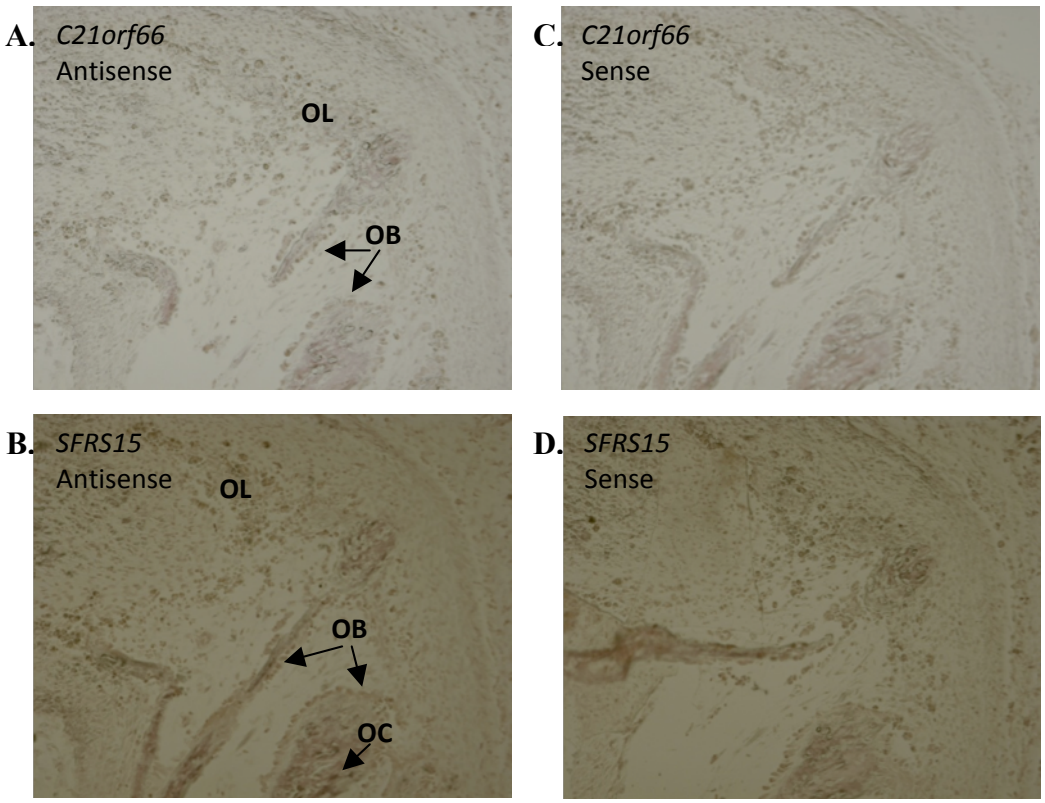

Figure 4.10. Brightfield micrographs of the localization of bidirectional transcripts of *C21orf66* and *SFRS15* in frontal bone at d 60 of gestation. **A-B.** Hybridization of digoxigenin-labeled antisense probes to sense transcripts. **C-D.** Sense controls. **A.** *C21orf66*. Expression was detected in developing mesenchyme along the osteogenic layer of the pericranium and in osteoblasts lining the trabecular bone. **C.** *Anti-C21orf66*. Expression of the antisense transcript appeared to co-localize with the sense transcript. **B, D.** *SFRS15*. Expression was observed in developing mesenchyme, osteoblasts and osteocytes. OL = osteogenic layer, OB = osteoblasts, OC = osteocytes. (40X)

Both *C21orf59* and *C21orf62* were expressed in the osteoblasts of the frontal bone in a pattern that appears to line the trabecular bone (Figure 4.9). In addition, expression of *C21orf59* extended to the developing mesenchyme along the osteogenic layer, but there was minimal expression of *C21orf62* in the mesenchyme. At d 80, *C21orf62* was also expressed in the osteoclasts of the frontal bones (data not shown). There was no evidence of expression of *C21orf59* or *C21orf62* in endochondral bone formation.

Expression of *C21orf66* was detected in osteoblasts and developing mesenchyme along the osteogenic layer of the pericranium and *SFRS15* was detected in osteoprogenitors, osteoblasts osteocytes (Figure 4.10). However, based on the intensity of hybridization signals, the relative levels of expression of *C21orf66* and *SFRS15* were lower at d 60 than *C21orf62* and *C21orf59*.

Expression of *C21orf66* and *SFRS15* was also detected in developing endochondral bone. At d 40 and 55, there was abundant expression of both genes within the cartilage of the femur, knee, and ear. At d 55, expression in the ear was specifically localized to areas of hyaline cartilage for both genes and there appeared to be a gradient of expression with less signal detected in regions distal to the cartilage (Figures 4.11 and 4.12).

Colocalization of these 4 genes from the polled interval in developing intramembranous bones suggests that all of these genes have a role in cranial facial bone development. Both *C21orf66* and *SFRS15* may also have roles in endochondral ossification. Given their close proximity on BTA1, it may be that these genes are

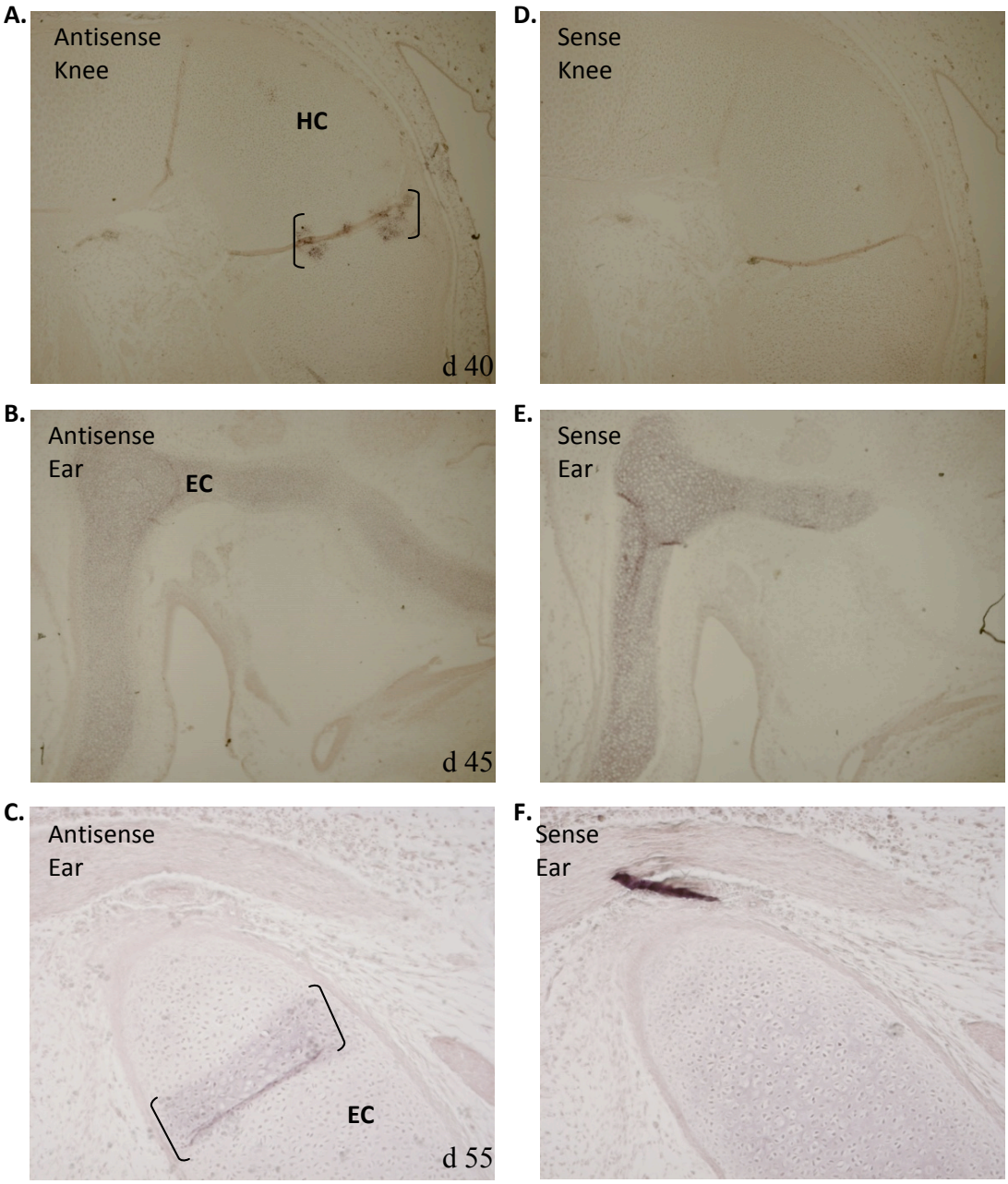

Figure 4.11. Brightfield micrographs of the localization of bidirectional transcripts of *C21orf66* in cartilage. **A-C.** Hybridization of digoxygenin-labeled antisense probes to sense transcripts. **C-E.** Detection of antisense transcripts with sense probes. **A, D.** Expression in the hyaline cartilage of the developing knee at d 40 of gestation (40x). Brackets indicate a gradient in expression. **B, E.** Expression in the elastic cartilage of the ear at d 45 (40x). **C, F.** Expression in the elastic cartilage of the ear at d 55 (100x). HC = hyaline cartilage, EC= elastic cartilage.

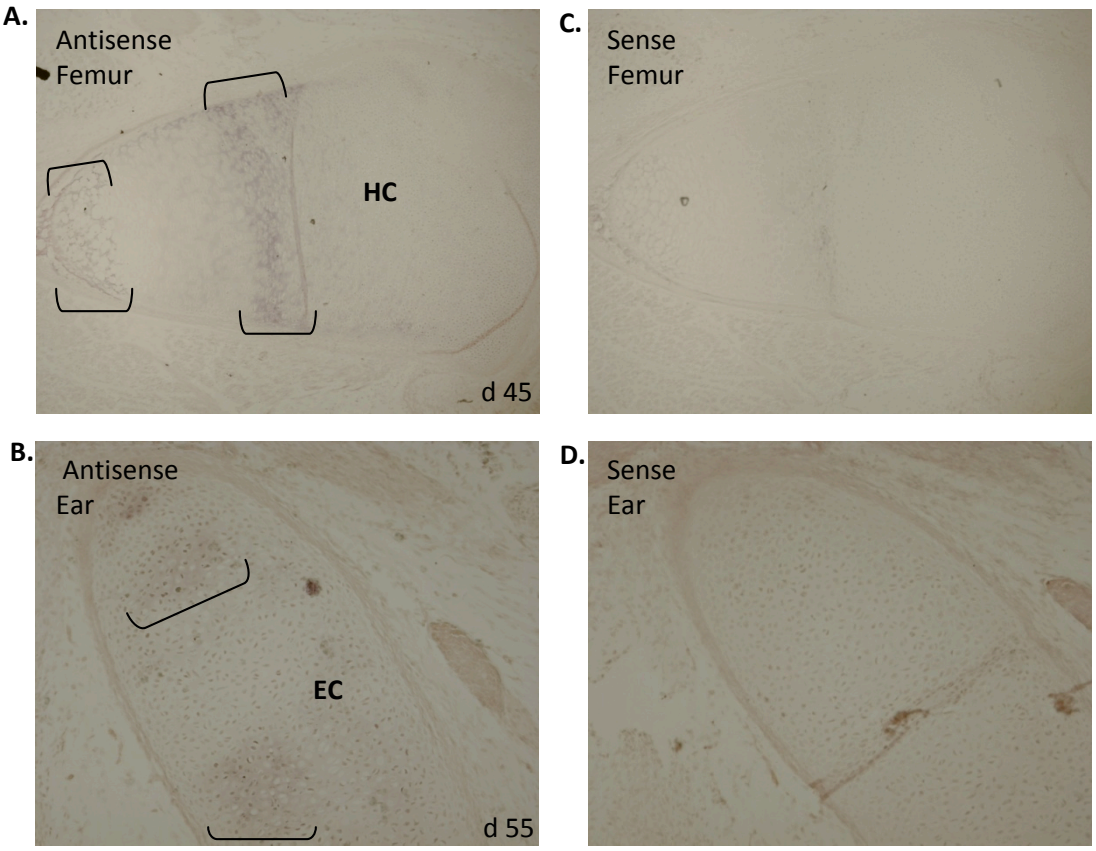

Figure 4.12. Brightfield micrographs of the localization of *SFRS15* in cartilage. **A-B.** Hybridization of digoxygenin-labeled antisense probes to sense transcripts. **C-D.** Sense control. **A, C.** Expression in the hyaline cartilage of the femur at the edge of the hypertrophic celss at d 45 of gestation. Brackets indicate a gradient in expression. **B, D.** Expression in the elastic cartilage of the ear at d 55. **C, F.** Expression in the elastic cartilage of the ear at d 55. (40x). HC = hyaline cartilage, EC= elastic cartilage.

coordinately regulated in some way. To the best of our knowledge, this is the first time that *in situ* hybridization data have suggested a role for any genes from the polled interval in bone development in any species.

4.5 Identification of Bovine C21orf66 *Antisense Transcripts*

Data collected by *in situ* hybridization were indicative of expression of an antisense transcript covering at least exons 12 and 13 of *C21orf66* in developing intramembranous and endochondral bone from d 45 to 55, and this had not previously been described for this gene in cattle. These data were verified by RT-PCR using cDNA from neonates synthesized with a gene-specific primer (C21orf66F; Table 3.2). There was also some evidence of an antisense transcript in the Genbank database in which there are 20 expressed sequences tags (EST) on the minus strand covering exons 12 to 18 and the 3' untranslated region of *C21orf66*. Presence of an antisense transcript for bovine *C21orf66* is also consistent with the finding by Huang et al. (2007), who demonstrated that there is an antisense transcript in human liver cells. As a result of confirming the presence of a *C21orf66* antisense transcript, the next objective was to determine the extent to which the *Anti-C21orf66* transcript was complementary to the *C21orf66* transcript.

Wunderlich (2008) predicted the existence of 2 *C21orf66* transcripts due to alternative splicing of exons 7 and 8 involving 131 bp from the end of intron 6 and 17 bp from the start of intron 9, respectively. To characterize the sense and antisense transcripts it was critical that gene-specific primers were utilized to synthesize cDNA because synthesis with random hexamers created a mixture of transcripts from both

strands. Amplification of each exon (or multiple exons simultaneously) was attempted from cDNA for the sense and antisense transcripts. The very high GC content of the 5' untranslated region and exon 1 made primer design difficult for that region. Sequence was obtained for exon 1 for the sense transcript but amplification failed from antisense cDNA. It was established that there are 2 sense transcripts for *C21orf66*. There was no evidence of the alternate exon 7 predicted by Wunderlich (2008) in the sense transcript. However, this alternate exon was present in the antisense transcript. There was also evidence of 2 antisense transcripts, one involving both alternate exon 7 and alternate exon 8 and the other involving just alternate exon 7. Although no sequence was produced for exon 18, this exon is represented in the antisense EST in Genbank. Gene models for the sense and antisense transcripts for bovine *C21orf66* are shown in Figure 4.13.

Sequences from the transcripts were aligned to genomic sequences produced by Wunderlich (2008) utilizing a panel of animals from horned and polled breeds. No new sequence variants were identified.

The sequence data collected suggest that the antisense transcript likely corresponds to the full sense transcript, with the exception of exons 7 and 8. The extent to which full-length natural antisense transcripts exist and their specific regulatory roles has yet to be widely reported (Kramer et al., 2003; Chen et al., 2005; Petit et al., 2009). Co-expression in the same cells, as was observed for *C21orf66*, and/or an inverse relationship between sense and antisense accumulation is indicative of regulation by the

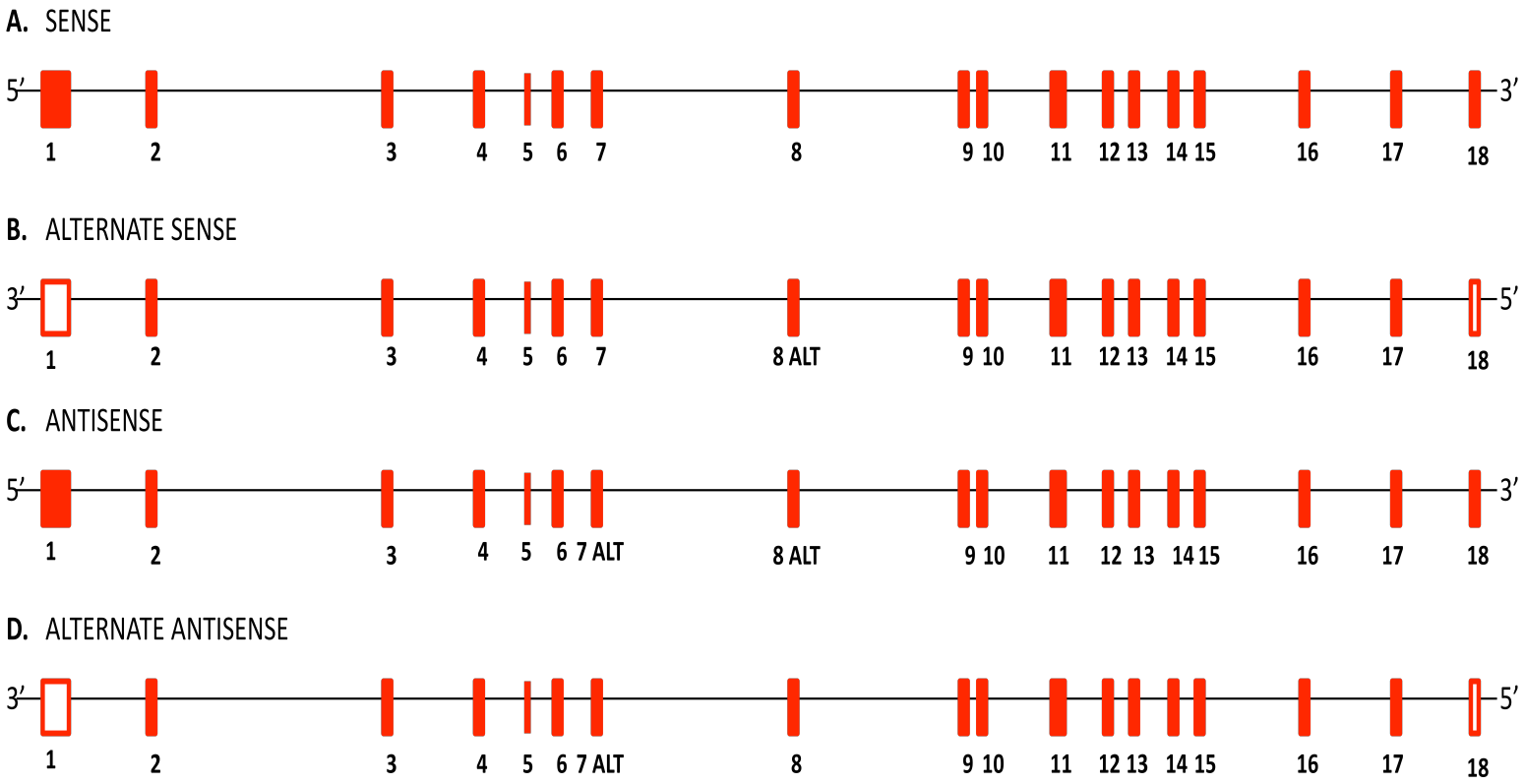

Figure 4.13. Map of exons in the *C21orf66* sense and antisense transcripts. Numbered boxes indicate the location of exons and sequence was generated for those that are solid red. **A.** Sense transcript. **B.** Alternate sense transcript. **C.** Antisense transcript. **D.** Alternate antisense transcript. Alternate transcripts are due to alternative splicing of exons 7 and 8.

antisense transcript (Chen et al., 2005). One example of a gene for which a fully complementary antisense transcript exists is canine erythropoietin receptor (EPO-R), and coordinate regulation of the sense and antisense EPO-R transcripts appears to be critical for lung growth (Zhang et al., 2008).

In this study, *MSX1* was shown to have an antisense transcript in cattle. This is similar to *MSX1* in mice, rats, and humans, for which an antisense transcript covering exon 2 of the sense transcript and part of the intron is expressed in differentiated bone and the balance of the levels of the 2 transcripts is related to the expression of MSX1 protein (Blin-Wakkach et al., 2001).

The role of the sense and antisense transcripts of *C21orf66* in intramembranous bone formation could be elucidated in vitro by perturbating the relative levels of the complementary transcripts and monitoring subsequent up- or down-regulation of other genes that are critical for bone formation.

5. SUMMARY AND CONCLUSIONS

The objective of this study was to conduct a survey of gene expression in bovine fetal samples at various stages of development for genes in the region on bovine chromosome 1 (*IFNAR1* to *SOD1*) known to contain the locus that causes horns, along with other genes with known roles in the osteogenesis and chrondrogenesis pathways. Our hypothesis was that the gene that determines the presence of horns is expressed in osteoprogenitor cells of the early fetus and will affect the expression of *RUNX2*, *MSX1*, *MSX2*, and/or *TWIST1*. Therefore gene expression was evaluated by both qualitative and quantitative RT-PCR and by in situ hybridization.

With the exception of *OLIG1*, which was only expressed in the brain, all of the genes investigated were expressed in fetal frontal and parietal bones by qualitative RT-PCR. When evaluated by realtime RT-PCR the level of expression of *C21orf59*, *C21orf66*, *IL10RB*, and *SFRS15* was observed to increase in the frontal bone of horned samples from d 55 to d 70 of gestation.

At d 60 of gestation a change in the shape of the frontal bone was observed, which has been reported to be the developmental stage when the horn bud appears. At this time point, genes with known roles in osteogenesis and chondrogenesis (*MSX1*, *TWIST1*, *RUNX2* and *SOX9*) were detected in frontal bone in cells from the osteoblast lineage as expected. Furthermore, *C21orf59*, *C21orf62*, *C21or66* and *SFRS15* from the polled interval were localized to developing mesenchyme, osteoblasts and/or osteoclasts of the frontal bone, suggesting that each of these genes has a role in intramembranous bone formation. In addition, gradients of expressed *C21orf66* and *SFRS15* were

detected in developing endochondral bone. Unexpectedly, there was evidence of an antisense transcript of *C21orf66* expressed in the same cell types as the sense transcript. Further characterization of this antisense transcript demonstrated that it covered the entire sense transcript.

A model of the possible roles of *C21orf59*, *C21orf62*, *C21orf66* and its antisense transcript, and *SFRS15* in intramembranous bone formation is presented in Figure 4.14. Both fibroblast growth factor (FGF) and BMP are important precursors for osteoblast differentiation. Distal-less homeobox 5 (DLX5) and RUNX2 are major regulators of bone differentiation. It is known that BMP2 regulates DLX5, which is required for expression of RUNX2, and FGF and BMP are important for the expression of MSX1, MSX2, and TWIST1 in normal differentiation. Mutations in the FGF and BMP pathways or in associated transcription factors result in skull malformations. Based on observed expression in the mesenchyme, rather than just in mature osteoblasts or osteoclasts, *C21orf66* and/or its antisense transcript become the most likely candidates for the polled locus. However, a mutation that disrupts expression of any of these genes would be expected to detrimentally affect intramembranous bone formation and could therefore prevent the development of horns.

A limitation of the current study was that fetal samples were collected from commercial cows without knowledge of their expected genotype at the polled locus. Future research that builds upon the data collected herein will require producing fetuses bred to be horned, polled or scurred. It is expected that expression patterns of genes (*OLIG2, C21orf49, TCP10L, C21orf77*, and *SOD1*) from the polled interval that were

not investigated herein will be characterized in future studies. In addition, quantitative RT-PCR and/or in situ hybridization must be completed for *C21orf63*, *HUNK*, *IFNAR1*, *IFNAR2*, *MRAP*, *C21orf45*, and *IL10RB*. *In vitro* expression assays that enable relative levels of expression of genes from the polled interval to be perturbated will help elucidate the role of these genes in intramembranous or endochondral bone formation and the development of horns in cattle.

A.

Mesenchymal condensations	Osteoprogentor cells	Osteoblasts	Osteocytes
s/asMSX1		s/asMSX1	s/asMSX1
TWIST1		TWIST1	TWIST1
s/asC21orf66	s/asC21orf66	s/asC21orf66	
	RUNX2	RUNX2	
	SFRS15	SFRS15	SFRS15
		C21orf59	
		C21orf62	
		SOX9	

B.

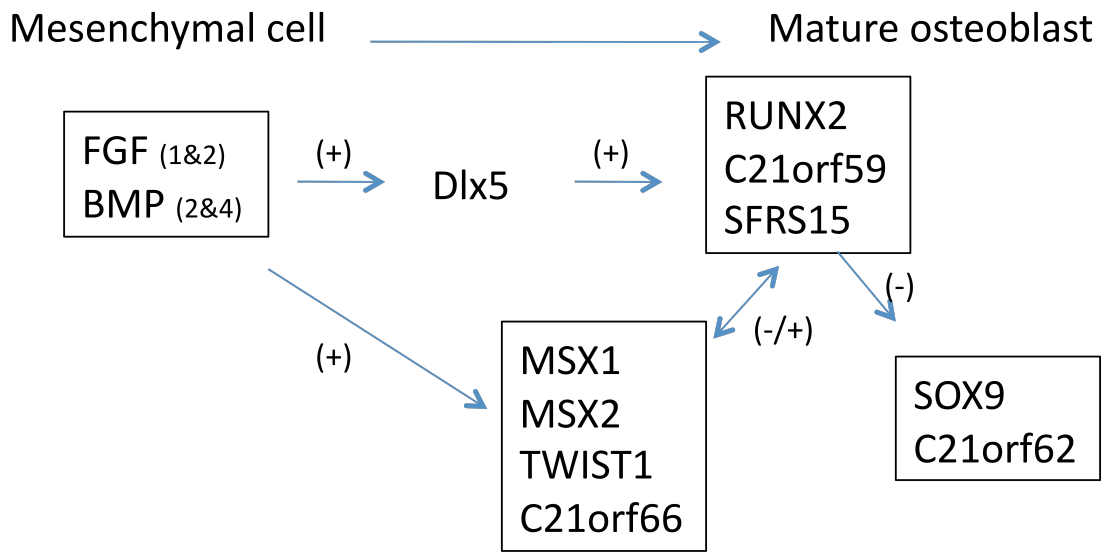

Figure 4.14. Model of the role of genes from the polled interval in intramembranous bone formation. **A.** Observed expression of genes classified by cell type. **B.** Schematic model showing how genes from the polled interval (*C21orf66*, *C21orf59*, *SFRS15*, and *C21orf62*) may interact with other signaling factors during osteoblast differentiation. s = sense, as = antisense.

LITERATURE CITED

Abzhanov, A., S. J. Rodda, A. P. McMahon, and C. J. Tabin. 2007. Regulation of skeletogenic differentiation in cranial dermal bone. Development 134: 3133-3144.

Antonopoulou, I., L. A. Mavrogiannis, A. O. Wilkie, and G. M. Morriss-Kay. 2004. Alx4 and Msx2 play phenotypically similar and additive roles in skull vault differentiation. J. Anat. 204: 487-499.

Asai, M., T. G. Berryere, and S. Schmutz. 2004. The scurs locus in cattle maps to bovine chromosome 19. Anim. Genet. 35: 34-39.

Bi, W., J. M. Deng, Z. Zhang, R. R. Behinger, and B. de Crombrugghe. 1999. *Sox9* is required for cartilage formation. Nat. Genet. 22: 85-89.

Blin-Wakkach, C., F. Lezot, S. Ghoul-Mazgar, D. Hotton, S. Monteiro, C. Teillaud, L. Pibouin, S. Orestes-Cardoso, P. Papagerakis, M. Macdougall, B. Robert, and A. Berdal. 2001. Endogenous Msx1 antisense transcript: In vivo and in vitro evidences, structure, and potential involvement in skeleton development in mammals. Proc. Natl. Acad. Sci. U. S. A. 98: 7336-7341.

Buchanan Smith, A.D. 1927. The inheritance of horns in cattle. Some further data. J. Genet. 18: 365-374.

Chen, J., M. Sun, L. D. Hurst, G. G. Carmichael, and J. D. Rowley. 2005. Genome-wide analysis of coordinate expression and evolution of human cis-encoded sense-antisense transcripts. Trends Genet. 21: 326-329.

Cheng, X., Y. Wang, Q. He, M. Qiu, S. R. Whittemore, and Q. Cao. 2007. Bone morphogenetic protein signaling and Olig1/2 interact to regulate the differentiation and maturation of adult oligodendrocyte precursor cells. Stem Cells 25: 3204-3214.

Connerney, J., V. Andreeva, Y. Leshem, M. A. Mercado, K. Dowell, X. Yang, V. Lindner, R. E. Friesel, and D. B. Spicer. 2008. Twist1 homodimers enhance FGF responsiveness of the cranial sutures and promote suture closure. Dev. Biol. 318: 323-334.

Davis, S.L.F., J.F. Taylor, D.R. Stillwell, C.A. Gill, and S.K. Davis. 1999. Comparative sequence analysis of the Down syndrome critical region in humans and cows identifies genes encoding rare transcripts. Page 88 in Proceedings of the Genome Mapping, Sequencing and Biology meeting, Cold Spring Harbor, NY.

de Crombrugghe, B., V. Lefebvre, and K. Nakashima. 2001. Regulatory mechanisms in the pathways of cartilage and bone formation. Curr. Opin. Cell Biol. 13: 721-727.

Dove, F. A. 1935. The physiology of horn growth: A study of the morphogenesis, the interaction of tissues, and the evolutionary processes of a Mendelian recessive character by means of transplantation of tissues. J. Exp. Zool. 69: 347-405.

Ducy, P., R. Zhang, V. Geoffroy, A. L. Ridall, and G. Karsenty. 1997. Osf2/Cbfa1: A transcriptional activator of osteoblast differentiation. Cell 89: 747-757.

Evans, H. E., and W. O. Sack. 1973. Prenatal development of domestic and laboratory mammals: Growth curves, external features and selected references. Zentralbl. Veterinarmed. C. 2: 11-45.

Fambach, O. 1901. Untersuchungan und Beobachtungen uber das os cornu. Zeitschr. F. Naturwiss. 74: 1-16. Translated by S. Hiendleder, 2008.

Francis-West, P., R. Ladher, A. Barlow, and A. Graveson. 1998. Signalling interactions during facial development. Mech. Dev. 75: 3-28.

Gadow, H. 1902. The evolution of horns and antlers. Proc. Zool. Soc. London Pt. 1: 206-222.

Georges, M., R. Drinkwater, T. King, A. Mishra, S. S. Moore, D. Nielsen, L. S. Sargeant, M. R. Steele, X. Zhao, J. E. Womack, and J. Hetzel. 1993. Microsatellite mapping of a gene affecting horn development in *Bos taurus*. Nat. Genet. 4: 206-210.

Goonewardene, L. A., and R. K. Hand. 1991. Studies on dehorning steers in Alberta feedlots. Can. J. Anim. Sci. 71: 1249-1252.

Goonewardene, L. A., M. A. Price, M. F. Liu, R. T. Berg, and C. M. Erichsen. 1999. A study of growth and carcass traits in dehorned and polled composite bulls. Can. J. Anim. Sci. 79: 383-385.

Han, J., M. Ishii, P. Bringas, Jr., R. L. Maas, R. E. Maxson, Jr., and Y. Chai. 2007. Concerted action of Msx1 and Msx2 in regulating cranial neural crest cell differentiation during frontal bone development. Mech. Dev. 124: 729-745.

Hill, R. E., P. F. Jones, A. R. Rees, C. M. Sime, M. J. Justice, N. G. Copeland, N. A. Jenkins, E. Graham, and D. R. Davidson. 1989. A new family of mouse homeo box-containing genes: Molecular structure, chromosomal location, and development expression of Hox-7.1. Genes Dev. 3: 26-37.

Hoffsis, G. 1995. Surgical (cosmetic) dehorning in cattle. Vet. Clin. Food Anim. 11: 159-169.

Holleville, N., S. Mateos, M. Bontoux, K. Bollerot, and A. H. Monsoro-Burq. 2007. Dlx5 drives Runx2 expression and osteogenic differentiation in developing cranial suture mesenchyme. Dev. Biol. 304: 860-874.

Huang, J., P. Hao, Y. L. Zhang, F. X. Deng, Q. Deng, Y. Hong, X. W. Wang, Y. Wang, T. T. Li, X. G. Zhang, Y. X. Li, P. Y. Yang, H. Y. Wang, and Z. G. Han. 2007. Discovering multiple transcripts of human hepatocytes using massively parallel signature sequencing (MPSS). BMC Genomics 8: 207.

Ishii, M., A. E. Merrill, Y. S. Chan, I. Gitelman, D. P. Rice, H. M. Sucov, and R. E. Maxson, Jr. 2003. Msx2 and Twist cooperatively control the development of the neural crest-derived skeletogenic mesenchyme of the murine skull vault. Development 130: 6131-6142.

Kerr, J. B. 1999. Atlas of functional histology. Mosby, Inc., London.

Kierszenbaum, A. L. 2002. Histology and cell biology. Mosby, Inc., St. Louis.

Kramer, C., J. J. Loros, J. C. Dunlap, and S. K. Crosthwaite. 2003. Role for antisense RNA in regulating circadian clock function in *Neurospora crassa*. Nature 421: 948-952.

Lana-Elola, E., R. Rice, A. E. Grigoriadis, and D. P. Rice. 2007. Cell fate specification during calvarial bone and suture development. Dev. Biol. 311: 335-346.

Livak, K. J., and T. D. Schmittgen. 2001. Analysis of relative gene expression data using real-time quantitative pcr and the 2(-delta delta c(t)) method. Methods 25: 402-408.

Long, C. R., and K. E. Gregory. 1978. Inheritance of the horned, scurred, and polled conditions in cattle. J. Hered. 69: 395-400.

McKenna, D. R., D. L. Roeber, P. K. Bates, T. B. Schmidt, D. S. Hale, D. B. Griffin, J. W. Savell, J. C. Brooks, J. B. Morgan, T. H. Montgomery, K. E. Belk, and G. C. Smith. 2002. National Beef Quality Audit-2000: Survey of targeted cattle and carcass characteristics related to quality, quantity, and value of fed steers and heifers. J. Anim. Sci. 80: 1212-1222.

Noden, D. M. 1983. The role of the neural crest in patterning of avian cranial skeletal, connective, and muscle tissue. Dev. Biol. 96: 144-165.

Ornitz, D. M., and P. J. Marie. 2002. FGF signaling pathways in endochondral and intramembranous bone development and human genetic disease. Genes Dev. 16: 1446-1465.

Otto, F., A. P. Thornell, T. Crompton, A. Denzel, K. C. Gilmour, I. R. Rosewell, G. W. H. Stamp, R. S. P. Beddington, S. Mundlos, B. R. Olsen, P. B. Selby, and M. J. Owen. 1997. *Cbfa1*, a candidate gene for Cleidocranial Dysplasia Syndrome, is essential for osteoblast differentiation and bone development. Cell 89: 765-771.

Petit, S., F. Meary, L. Pibouin, J. C. Jeanny, I. Fernandes, A. Poliard, D. Hotton, A. Berdal, and S. Babajko. 2009. Autoregulatory loop of Msx1 expression involving its antisense transcripts. J. Cell. Physiol. 220: 303-310.

Rice, D. P. C., T. Åberg, Y.-S. Chan, Z. Tang, P. J. Kettunen, L. Pakarinen, R. E. Maxson, Jr., and I. Thesleff. 2000. Integration of FGF and TWIST in calvarial bone and suture development. Dev. Biol. 127: 1845-1855.

Richardson, C., V. Barnard, P. C. Jones, and C. N. Hebert. 1991. Growth rates and patterns of organs and tissues in the bovine fetus. Br. Vet. J. 147: 197-206.

Smith, G. C., J. W. Savell, J. B. Morgan, and T. E. Lawrence. 2006. Report of the June-September, 2005 National Beef Quality Audit: A new benchmark for the U. S. beef industry. Pages 5-11 in Proceedings of the 38th annual meeting of the Beef Improvement Federation, Choctaw, MS.

Soo, K., M. P. O'Rourke, P. L. Khoo, K. A. Steiner, N. Wong, R. R. Behringer, and P. P. L. Tam. 2002. Twist function is required for the morphogenesis of the cephalic neural tube and the differentiation of the cranial neural crest cells in the mouse embryo. Dev. Biol. 247: 251-270.

Stein, G. S., J. B. Lian, A. J. van Wijnen, J. L. Stein, M. Montecino, A. Javed, S. K. Zaidi, D. W. Young, J.-Y. Choi, and S. M. Pockwinse. 2004. Runx2 control of organization, assembly and activity of the regulatory machinery for skeletal gene expression. Oncogene 23: 4315-4329.

White, W. T., and H. L. Ibsen. 1936. Horn inheritance in Galloway-Holstein cattle crosses. J. Genet. 11: 59-67.

Wunderlich, K. R. 2008. Structural and functional characterization of the polled interval on bovine chromosome 1. Ph.D. Dissertation. Texas A&M University, College Station, TX.

Yamashiro, T., X.-P. Wang, Z. Li, S. Oya, T. Åberg, T. Fukunaga, H. Kamioka, N. A. Speck, T. Takano-Yamamoto, and I. Thesleff. 2004. Possible roles of Runx1 and Sox9 in incipient intramembranous ossification. J. Bone Miner. 19: 1671-1677.

Yoshida, T., L. A. Phylactou, J. B. Uney, I. Ishikawa, K. Eto, and S. Iseki. 2005. Twist is required for establishment of the mouse coronal suture. J. Anat. 206: 437-444.

Zhang, Q., J. Zhang, O. W. Moe, and C. C. Hsia. 2008. Synergistic upregulation of erythropoietin receptor (EPO-R) expression by sense and antisense EPO-R transcripts in the canine lung. Proc. Natl. Acad. Sci. U. S. A. 105: 7612-7617.

APPENDIX A

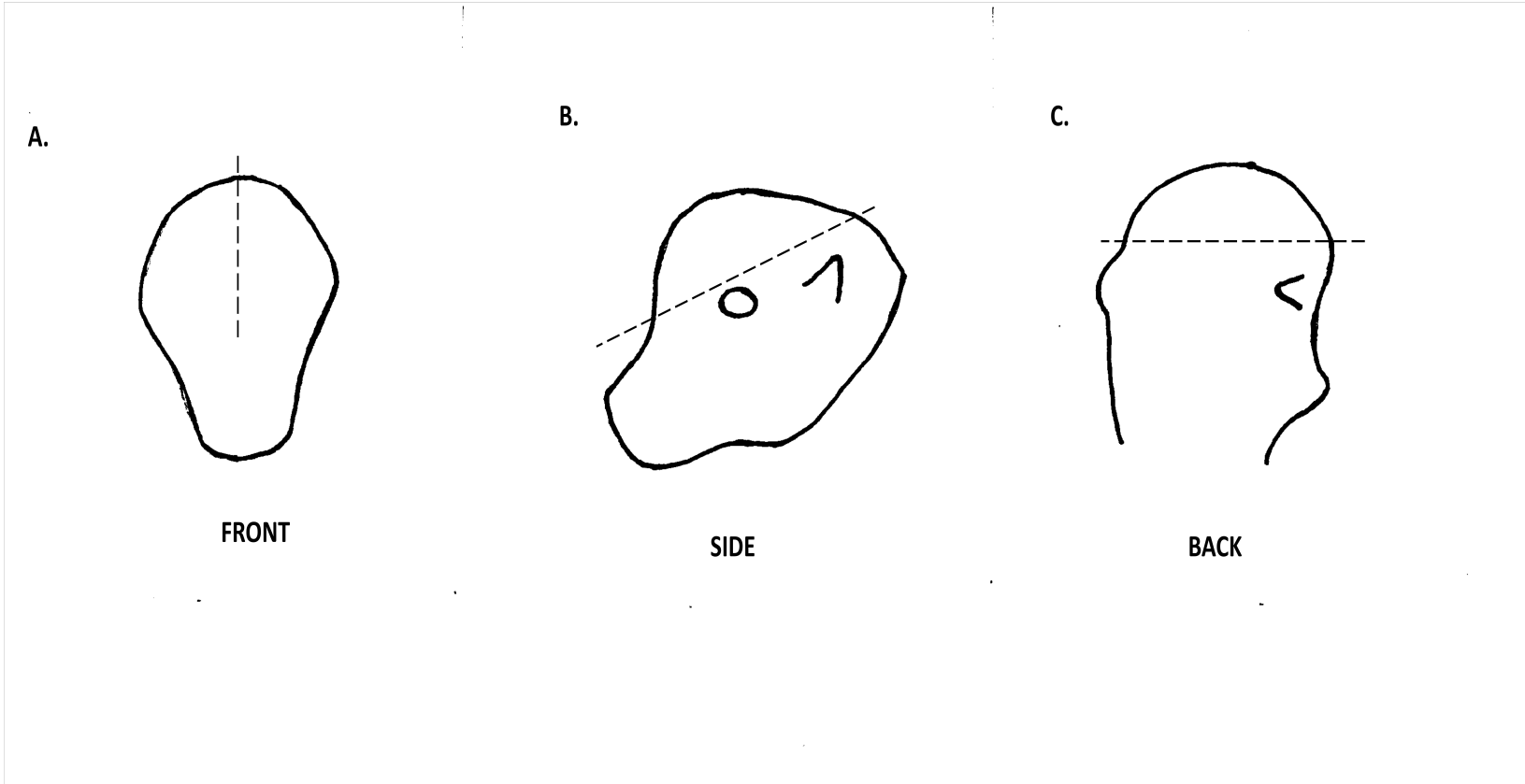

Figure A.1. Fetal dissection for RNA extraction. **A.** First incision was made between the frontal bones from the nasal bone cutting posteriorly to the occipital condyle. **B.** Second incision was made from the nasal bone continuing posteriorly above the eye and ear, meeting the first incision at the occipital condyle. **C.** The top portion of the head was removed just above the ear.

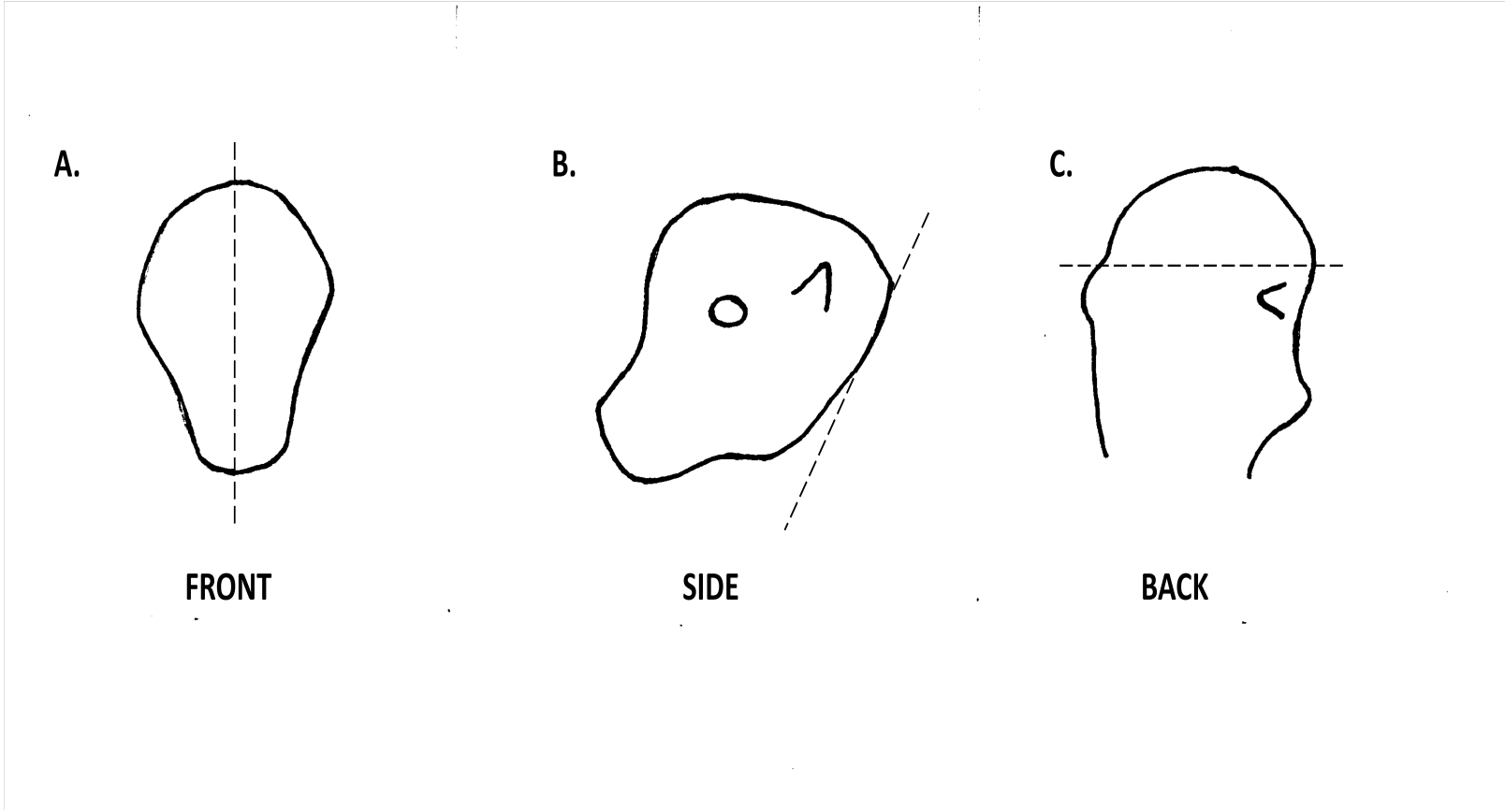

Figure A.2. Fetal dissection for histology. **A.** First incision is made between the frontal and nasal bones splitting the head. **B.** Second incision is made at the occipital condyle to remove the head. **C.** For analysis of the top portion of the head, an incision was made just above the ear continuing to the front just above the eyes.

APPENDIX B

Table B.1. Nomenclature of genes located in the polled interval and genes involved in osteogenesis and chondrogenesis.

Role	Gene Name[1]	Symbol[1]	HSA[1,2]
Polled Interval	chromosome 21 open reading frame 45	*C21orf45*	21q22.11
	chromosome 21 open reading frame 59	*C21orf59*	21q22.1
	chromosome 21 open reading frame 62	*C21orf62*	21q22.1
	chromosome 21 open reading frame 63	*C21orf63*	21q22.11
	chromosome 21 open reading frame 66	*C21orf66*	21q22.11
	interleukin 10 receptor, beta	*IL10RB*	21q22.1-q22.2
	splicing factor, arginine/serine-rich 15	*SFRS15*	21q22.1
	synaptojanin 1	*SYNJ1*	21q22.2
	hormonally up-regulated Neu-associated kinase	*HUNK*	21q22.1
	interferon (alpha, beta and omega) receptor 1	*IFNAR1*	21q22.1
	interferon (alpha, beta and omega) receptor 2	*IFNAR2*	21q22.1
	melanocortin 2 receptor accessory protein	*MRAP*	21q22.1
	oligodendrocyte transcription factor 1	*OLIG1*	21q22.11
Osteogenesis/ Chondrogenesis	bone morphogenetic protein 4	*BMP4*	14q22-q23
	bone morphogenetic protein 7	*BMP7*	20q13
	fibroblast growth factor receptor 2	*FGFR2*	10q25.3-q26
	c-fos induced growth factor (vascular endothelial growth factor D)	*FIGF*	Xp22.31
	msh homeobox 1	*MSX1*	4p16.2
	msh homeobox 2	*MSX2*	5q35.2
	runt-related transcription factor 1	*RUNX1*	21q22.3
	runt-related transcription factor 2	*RUNX2*	6p21

Table B.1 continued.

Role	Gene Name[1]	Symbol[1]	HSA[1,2]
Osteogenesis/ Chondrogenesis	protein kinase, cAMP-dependent, catalytic, alpha	*PRKACA*	19p13.1
	SRY (sex determining region Y)-box 9	*SOX9*	17q23
	twist homolog 1 (Drosophila)	*TWIST1*	7p21
	twist homolog 2 (Drosophila)	*TWIST2*	2q37.3
	signal transducer and activator of transcription 1, 91kDa	*STAT1*	2q32.2-q32.3
	parathyroid hormone-like hormone	*PTHLH*	12p12.1-p11.2
	forkhead box	*FOXL2*	3q23
	gremlin 1, cysteine knot superfamily, homolog (Xenopus laevis)	*GREM1*	15q13.3
	collagen, type XVIII, alpha 1	*COL18A1*	21q22.3
	cysteine-rich, angiogenic inducer, 61	*CYR61*	1p22.3
	glyceraldehyde-3-phosphate dehydrogenase	*GAPD*	12p13.31
	tyrosine 3-monooxygenase/tryptophan 5-monooxygenase activation protein, zeta polypeptide	*YWHAZ*	8q22.3

[1] From HUGO gene nomenclature.
[2] Human chromosome

VITA

Name: Sarah M. Vitanza

Address: Sarah Vitanza
7039 Deep Well Rd
Bryan, TX 77808

Email Address: svitanza357@yahoo.com

Education: B.S., Animal Science, Texas A&M University, 2007
M.S., Animal Science, Texas A&M University, 2009